THE ASTROPHYSICAL JOURNAL, 336:152–172, 1989 January 1

IRAS[1] OBSERVATIONS OF A LARGE SAMPLE OF NORMAL IRREGULAR GALAXIES

DEIDRE A. HUNTER
Department of Terrestrial Magnetism, Carnegie Institution of Washington; and Lowell Observatory

JOHN S. GALLAGHER III
Kitt Peak National Observatory, National Optical Astronomy Observatories;[2] and Lowell Observatory

WALTER L. RICE
Jet Propulsion Laboratory, California Institute of Technology

AND

FRED C. GILLETT
Kitt Peak National Observatory, National Optical Astronomy Observatories[2]
Received 1988 March 11; accepted 1988 June 21

ABSTRACT

The rarity of dark nebulae in irregular galaxies and the low optical internal reddenings of these galaxies as compared with spiral galaxies suggest a deficiency of dust and are puzzling features of irregulars actively forming stars. In order to explore the dust content in irregular galaxies, we present far-infrared *IRAS* 12, 25, 60, and 100 μm observations for a large sample of these systems. Dwarf, giant, and amorphous irregulars have similar infrared properties. The low $L_{IR}/L_{H\alpha}$ ratios of these irregular galaxies are consistent with the irregulars being relatively transparent systems without large amounts of hidden star formation. Thus, $L_{H\alpha}$ is a good measure of the current massive star formation. Compared with spirals, the irregulars have similar L_{IR}/L_B ratios, warmer S_{100}/S_{60} ratios, cooler S_{25}/S_{12} ratios, lower $L_{IR}/L_{H\alpha}$ ratios, and lower dust–to–H I gas mass ratios. The temperature, dust–to–H I gas mass ratios, and L_{IR}/L_B ratios do not correlate with the metallicity of the ionized gas of the irregular galaxies. Distant luminous blue irregular galaxies stand out as having infrared-to-optical flux ratios which are consistent with higher optical thicknesses. These galaxies are also often interacting with other systems.

It is hard to disentangle sources of dust heating, such as the general interstellar radiation field and very young stars, from global infrared measurements. This is especially true when the global optical properties themselves are correlated as they are in constant star-formation rate systems. Nevertheless, simple models are presented for two primary sources of heating of dust—H II regions and the UV-dominated general interstellar radiation field. A sample of H II–dominated irregulars is identified, and model $L_{IR}/L_{H\alpha}$ and S_{100}/S_{60} ratios are found to agree fairly well with the observations. Irregulars have warmer dust compared with spirals because of their higher UV surface brightnesses and lower optical depths.

Star-formation rates derived from L_{IR} Tinsley-Renzini population models are also discussed. L_{IR} is a star-formation rate indicator because a variety of stellar population age groups can contribute to L_{IR}. Combining IR and optical star-formation rate indicators, we find that normal irregulars are generally not evolving via bursts of star formation, while some amorphous systems may be. The star-formation histories of luminous irregular galaxies are confused by optical depth effects, but many of these systems are in phases of enhanced star-forming activity.

Subject headings: galaxies: interstellar — galaxies: photometry — nebulae: H II regions — stars: formation

I. INTRODUCTION

The apparent dearth of dark nebulae and the low optical internal reddenings of many irregular (Irr) galaxies relative to spiral galaxies are puzzling features of actively star-forming Irr's. In spirals, star-forming regions are often quite dusty, and dust lanes often punctuate the disks, while Irr galaxies seem to contain relatively few dark nebulae. The issues of the dust content and dust properties of galaxies are important, since theoretical models indicate that galactic dust characteristics will affect the local star-formation process (Wolfire and Cassinelli 1987). Yet Irr's can be quite successful at forming stars, and the star-forming regions and their products appear to be relatively normal (cf. Hunter and Gallagher 1986). In order to explore this quandary and the role of the dust in Irr galaxies, in an earlier paper Hunter *et al.* (1986) presented far-infrared (FIR) *IRAS* 12, 25, 60, and 100 μm observations of a small sample of Irr's chosen to span a range in overall level of star-formation activity. In this paper we continue the investigation into the nature of the dust in Irr's with a much larger sample of *IRAS* observations of Irr galaxies.

The program galaxies were chosen from the list of Hunter and Gallagher (1986), and their subgroupings of the Irr's will be retained here. The Irr's are divided into four subgroups: (1) The "dwarf" Irr's are Magellanic-type Irr's of low stellar surface brightness. These systems come primarily from van den Bergh's (1959) survey. (2) "Giant" Irr's are the high surface brightness cousins of the dwarfs. (3) The "amorphous" Irr's are noted for their smoothness and lack of resolution into stars and star clusters (Sandage and Brucato 1979). (4) Finally, the

[1] This research was supported in part under NASA's *IRAS* Data Analysis Program and funded through the Jet Propulsion Laboratory.
[2] Operated by the Association of Universities for Research in Astronomy, Inc., under contract with the National Science Foundation.

"distant" Irr's include systems referred to as luminous blue galaxies (LBGs) or clumpy Irr's.

These groups of Irr's have many similar properties which are summarized and compared by Hunter and Gallagher (1986). The similarities include properties such as *UBV* colors, stellar population characteristics, surface brightness, luminosity, mass, rotation, metallicity, fraction of the galaxian mass in gas, star-formation rates (SFRs) per unit area, time scales to exhaust the gas at the current rates, and SFR per unit blue stellar luminosity. However, there are some important differences. The dwarf Irr's are distinguished from the giant Irr's purely on the basis of surface brightness and different from the giant Irr's only in the overall level of star-formation activity and in parameters, such as surface brightness, which are a consequence of the level of star formation (Hunter and Gallagher 1985*a*). The dwarfs and giants are normal, nearby, noninteracting disk systems which are evolving at constant rates (Gallagher, Hunter, and Tutukov 1984).

The amorphous Irr's, on the other hand, although actively forming stars like the giant Irr's, are morphologically distinct. The amorphous systems lack the many star clusters of the Magellanic-type Irr's and often contain a single, centrally located supergiant H II region. They also show a wider scatter of *UBV* and $L_{H\alpha}/L_B$ properties which could be the result of greater variations in SFRs during the recent past as a consequence of the unusual spatial distributions of star-forming regions (Gallagher and Hunter 1987*b*). Some of these systems could be interacting, but most appear to be isolated.

The LBGs are more luminous and massive systems compared with the other groups of Irr's and are at such large distances that morphological distinctions and the elimination of interacting systems are more difficult. In fact, many of the LBGs are probably interacting with neighbors. The LBGs also tend to be more metal-rich compared with the other Irr's and to have higher rotation velocities (Gallagher, Hunter, and Bushouse 1989).

In §§ II and III we present the data. In § IV we discuss the problem of disentangling sources of dust heating and present simple two-component models. Section V is an application of these models to Irr galaxies. In § VI we discuss SFRs derived from L_{IR}, and § VII is a summary.

II. THE DATA

The *IRAS* instrumentation, operation, and calibration procedures are described by Neugebauer *et al.* (1984) and in the *IRAS Explanatory Supplement* (1985). The data were extracted from the archives at IPAC. Multiple survey scans covering each galaxy were co-added to produce both point-source–filtered and total flux surface brightness maps. For each galaxy profile, cuts were made through the surface brightness maps and were compared with those of a point source. Several objects were found to be extended relative to a point source as seen by *IRAS*, and for these objects fluxes were obtained from the surface brightness maps. For the rest of the galaxies the point-source–filtered maps were used.

The flux densities and uncertainties for the four *IRAS* passbands at 12, 25, 60, and 100 μm are listed in Tables 1 and 2. We have used the calibration as given in 1985 July, and the flux densities are color-corrected based on Planck fits to adjacent bands. A few objects were detected but not measurable because of confusion with other sources or cirrus. Upper limits are taken to be 3 times the median noise. The data given in Table 1 are expected to be of higher signal-to-noise ratio than those given in the *IRAS Point Source Catalog* (1985), and a comparison of these data without the color corrections is shown in Figure 1. One can see that at 12 and 25 μm the *Point Source Catalog* is systematically higher relative to the co-added data, while at 60 and 100 μm the co-added data generally yield higher fluxes.

Derived infrared properties and ratios with optical parameters are given in Table 3. The optical data and distances ($H_0 = 50$ km s^{-1} Mpc^{-1}) used in this paper are tabulated in Hunter and Gallagher (1986) and Gallagher, Hunter, and Bushouse (1989). $L_{H\alpha}$ for NGC 1705 is from Gallagher and Hunter (1987*b*). Hα and *B* luminosities are corrected for reddening in the Milky Way only (Burstein and Heiles 1984) unless otherwise noted. For comparison with spiral galaxies we have chosen objects from Kennicutt's (1983) list of Hα observations of spirals and have taken infrared data for the systems from the *Cataloged Galaxies and Quasars Observed in the IRAS Survey* (1985).

The *IRAS* fluxes presented here are galaxy-wide measurements of all dust radiating in these passbands. As such, the fluxes therefore integrate over many dust temperature components, analogous to the way in which multiple stellar temperature groups contribute to broadband *UBV* colors. Hunter *et al.* (1986), as a way to begin looking at the data, took the 12 and 25 μm fluxes to represent a warm component and the 60 and 100 μm fluxes to represent a cool component. Chini *et al.* (1986), on the other hand, have combined longer wavelength observations with the *IRAS* data for spirals and find that a warm dust component fits the *IRAS* 25 and 60 μm passbands and that a cool dust component contributes to the 100 μm band. The 12 μm flux did not fit either of these components. Separating the multiple dust components is not possible from the *IRAS* data alone, and this adds to the complexity of interpreting the data. In this paper, however, we will continue to use the definition of L_{IR} as $L_{IR} = \nu f_{80\,\mu m}$ and to compare galaxy dust color temperature contents through the ratios S_{25}/S_{12} and S_{100}/S_{60}, just as one compares stellar content among galaxies through use of $U-B$ and $B-V$ colors.

Throughout this paper, as well as in Hunter *et al.* (1986), galactic blue luminosities are based on standard optical definitions of in-band flux. Thus, $L_B = 7.81 \times 10^{34}$ dex $(-0.4M_B)$ ergs s^{-1}. This differs from the quasi-bolometric fluxes, defined by $f_B = \lambda_B f_\lambda(4400\ \text{Å})$ ergs s^{-1} cm^{-2}, which were used by de Jong *et al.* (1984). The quasi-bolometric fluxes are 4.5 times larger than the in-band fluxes. In § III, where we compare the Irr galaxy data with spirals from de Jong *et al.*, the spiral blue luminosities are corrected to the in-band quantity used here.

III. THE INFRARED AND OPTICAL PROPERTIES OF THE GALAXIES

a) Comparison among Groups of Irregulars

Histograms showing the number distributions for various infrared and optical ratios are shown in Figure 2, where one can see how the different groups of Irr's compare in these properties. Among the nearby, noninteracting groups of Irr's—the dwarfs, giants, and amorphous Irr's—the dwarfs tend to have lower L_{IR}/L_B ratios. Otherwise the groups are fairly well mixed in terms of the properties shown in Figure 2. There are, however, a few galaxies that stand out as unusual. NGC 1569 has an unusually high S_{25}/S_{12} ratio, indicating cooler dust (see also Hunter *et al.* 1986); II Zw 40 has a very high L_{IR}/L_B ratio; and DDO 47 has a cooler S_{100}/S_{60} temperature ratio and also stands out with a very high $L_{IR}/L_{H\alpha}$ ratio.

TABLE 1

IRAS FLUXES OF IRREGULAR GALAXIES

GALAXY	S_ν[a] (Jy)				UNCERTAINTY IN S_ν[b] (Jy)			
	12 μm	25 μm	60 μm	100 μm	12 μm	25 μm	60 μm	100 μm
Giants								
NGC 1012	0.27	0.32	5.76	9.05	0.05	0.05	0.9	1.4
NGC 1156	0.15	0.45	5.77	9.65	0.05	0.08	0.9	2.4
NGC 1569	0.88	8.55	48.90	54.80	0.1	1.1	7	8
NGC 3274[c]	≤0.05	≤0.05	1.14	1.95	...	...	0.2	0.3
NGC 3510	≤0.05	≤0.05	0.70	1.82	...	...	0.1	0.3
NGC 3738	≤0.05	0.09	2.28	3.96	...	0.03	0.4	0.6
NGC 3952	≤0.07	0.29	1.82	2.44	...	0.07	0.3	0.4
NGC 4214	0.35	1.74	16.38	29.71	0.07	0.3	2.5	4.4
NGC 4449	1.92	4.19	34.10	67.60	0.2	0.5	3	8
NGC 7292	≤0.05	≤0.04	1.45	2.83	...	...	0.2	0.4
NGC 7800	≤0.07	0.15	1.39	2.91	...	0.05	0.2	0.5
A1004+10	≤0.06	≤0.07	0.62	1.19	...	...	0.1	0.2
Dwarfs								
DDO 42	≤0.05	0.54	4.10	4.34	...	0.08	0.6	0.7
DDO 47	...	...	0.11	0.54	...	...	0.05	0.2
DDO 49	≤0.05	≤0.04	0.39	0.67	...	...	0.08	0.2
DDO 50	0.06	0.17	2.23	3.05	0.03	0.04	0.2	0.3
DDO 53	≤0.05	0.13	0.34	0.59	...	0.03	0.07	0.2
DDO 64	0.15	≤0.05	0.27	0.42	0.04	...	0.06	0.1
DDO 75	0.11	0.12	0.33	≤0.3	0.04	0.04	0.07	...
DDO 140	≤0.06	≤0.07	0.31	0.51	...	...	0.07	0.1
DDO 168	≤0.06	≤0.04	0.25	0.73	...	...	0.07	0.2
DDO 218	≤0.06	≤0.05	0.55	1.15	...	...	0.1	0.2
NGC 2552	≤0.05	≤0.04	0.80	1.59	...	...	0.1	0.3
Amorphous								
NGC 1140	0.19	0.39	3.94	5.00	0.05	0.07	0.6	0.8
NGC 1705	≤0.05	≤0.03	1.09	2.10	...	...	0.2	0.3
NGC 1800	≤0.04	≤0.03	1.02	1.87	...	...	0.2	0.3
NGC 4670	≤0.06	0.31	3.09	5.09	...	0.06	0.5	0.8
NGC 5253	3.19	10.47	30.91	31.07	0.5	1.6	4.6	4.6
Haro 22[d]	≤0.05	≤0.06	0.24	≤0.3	...	...	0.06	...
Mrk 35	0.26	0.89	5.92	7.57	0.05	0.2	0.8	1.1
II Zw 40	0.53	2.17	7.28	6.36	0.09	0.3	0.9	1.1
Distant								
Mrk 314	≤0.02	≤0.09	1.55	1.62	...	...	0.2	0.3
Mrk 390	≤0.06	≤0.06	0.70	1.14	...	...	0.1	0.2
Haro 15	≤0.06	≤0.06	1.60	2.17	...	...	0.2	0.3
Haro 20	≤0.05	0.11	0.37	0.60	...	0.03	0.07	0.2
II Zw 23	0.19	0.30	3.45	4.94	0.04	0.07	0.5	0.7
II Zw 33	≤0.05	≤0.04	0.67	≤0.3	...	...	0.1	...
II Zw 185[e]	≤0.05	≤0.04	0.66	≤0.3	...	...	0.1	...
III Zw 12	≤0.06	≤0.05	1.10	1.71	...	...	0.2	0.3
III Zw 33	≤0.06	≤0.07	0.69	≤0.4	...	...	0.1	...
III Zw 42	0.14	0.23	1.28	2.00	0.04	0.06	0.2	0.3
III Zw 43	≤0.07	0.43	3.12	3.59	...	0.09	0.5	0.5
IV Zw 149	0.12	0.49	5.53	7.37	0.04	0.08	0.8	1.1

NOTE.—Galaxies which are extended relative to a point source are NGC 4214, NGC 5253 (60 and 100 μm only), DDO 42 (= NGC 2366), and DDO 75 (= Sex A, 60 and 100 μm only). For these galaxies fluxes were extracted from the surface brightness maps. Values for DDO 47, DDO 50 (= Holmberg II, extended), NGC 4449 (extended), and II Zw 40 are from Hunter *et al.* 1986 and are corrected to the current calibration.

[a] The values of S_ν are color-corrected.

[b] Uncertainties are calculated from $(\sigma/f_\nu)^2 = 1/(\mathrm{S/N})^2 + (0.15)^2$, where 0.15 is the overall estimated uncertainty in the *IRAS* calibration and color corrections and the S/N is the median signal-to-noise ratio.

[c] The S_{25} position differed from that for 60 and 100 μm and was rejected.

[d] The S_{100} position differed and was rejected.

[e] S_{100} could not be deconvolved from a neighboring source.

TABLE 2

IRAS FLUXES OF SOURCES NEAR LBGs

Galaxy	Name	α(1950)	δ(1950)	d^a	S_ν (Jy) 12 μm	25 μm	60 μm	100 μm
Haro 15b	...	0h46m21s4	−13°22′14″	23′	≤0.06	≤0.06	≤0.15	0.95
Haro 20a	MCG 03-09-044	3 25 24.8	−17 10 43	26	≤0.04	≤0.03	0.65	1.82
Haro 20b	...	3 24 57.2	−17 29 08	16	≤0.04	≤0.03	0.28	0.87
Haro 20c	...	3 25 32.1	−17 33 44	7	≤0.04	≤0.03	0.17	≤0.3
Haro 20d	NGC 1345	3 27 17.0	−17 56 52	27	≤0.04	≤0.03	0.92	1.74
II Zw 33a	MCG 01-14-003	5 09 12.5	−3 09 07	28	≤0.05	0.17	1.63	≤0.3
II Zw 33b	MCG 01-14-004	5 09 14.2	−3 04 33	25	≤0.05	≤0.04	0.31	≤0.35
II Zw 33d	...	5 07 39.1	−2 26 45	20	≤0.05	≤0.04	0.46	≤0.3
II Zw 33f	...	5 07 56.3	−2 36 38	9	≤0.04	≤0.04	0.25	≤0.35
II Zw 185a	IC 5242	22 38 50.4	23 08 41	3	≤0.06	0.17	1.13	≤0.3
II Zw 185c	...	22 39 21.2	23 04 03	5	≤0.05	≤0.04	0.53	0.64
IV Zw 149a	...	23 24 59.7	23 22 28	5	≤0.06	0.12	0.84	≤0.3
IV Zw 149b	Mrk 326	23 25 36.9	23 15 23	4	0.28	0.65	4.54	6.33
III Zw 33a	III Zw 35	1 41 46.4	16 50 55	8	≤0.07	1.08	14.64	13.77
III Zw 33c	...	1 40 20.1	17 02 28	19	≤0.06	≤0.06	0.40	≤0.4

NOTE.—The S_{100} profiles for II Zw 33a–f are peculiarly elongated and were not measured. Furthermore, no color correction has been applied. The S_{100} profile of II Zw 185a is confused with that of the program galaxy.

[a] The parameter d is the projected distance on the sky between the program object and its neighbor.

Many of the LBGs, however, lie at the extremes of the distributions with respect to the other groups of Irr's. The LBGs tend to have higher ratios of $L_{IR}/L_{H\alpha}$ and L_{IR}/L_B and somewhat warmer S_{100}/S_{60} dust color temperatures (Klein *et al.* 1986). The survey data were extracted in maps 0°.5 × 1° centered on the object of interest. In examining these maps for each galaxy, the LBGs also stood out as having a much higher frequency of other point sources in the field of view. Among the 12 objects that we have classified as LBGs, six have other sources (often more than one) within the field which are nearly as strong or stronger than the program galaxy at 60 and 100 μm. Of the 32 other program Irr's, only five have even one other moderately strong source in the extracted field. The neighboring sources of the LBGs are given in Table 2. Some of the neighboring sources are identified as galaxies from a comparison with the Palomar Sky Survey, but CCD images of a few "blank" source positions have also revealed galaxies. An examination of the Palomar Sky Survey around Haro 15 further shows many blue galaxies over a large region. The heightened frequency of nearby sources is consistent with the suggestion by Gallagher, Hunter, and Bushouse (1989) that many of the distant, luminous, or clumpy Irr's are actually interacting systems. Thus, differences in the infrared properties of some of the LBGs could be due to the fact that these systems are interacting (see also Bushouse, Lamb, and Werner 1988).

It is interesting to note that many of the optical properties of the LBGs are not very different from those of the other groups of Irr's. Although oxygen abundances seem to be higher, optical spectra and *UBV* colors of LBGs are similar to those of the other Irr's; yet the infrared properties are significantly different. We will see in the next section that the converse situation also exists. The Irr and spiral galaxies have similar L_{IR}/L_B ratios in spite of different optical properties. Furthermore, the amorphous Irr's and Magellanic-type Irr's have different spatial distributions of star formation but similar optical and infrared properties. One can conclude, therefore, that infrared data are necessary to a thorough understanding of the properties of an actively star-forming galaxy.

The values of $L_{IR}/L_{H\alpha}$ seen in Figure 2 for the nearby Irr galaxy sample are relatively low; the median value is about 70. These values are consistent with the expectation that the nearby Irr galaxies are relatively transparent systems and that there is not a large amount of optically invisible star formation taking place in these galaxies (Hunter *et al.* 1986; Thronson and Telesco 1986). Thus, the value of $L_{H\alpha}$ is a good measure of the current star-formation activity in most nearby Irr galaxies.

b) *Comparison with Spirals*

Figure 3 is a plot of log (L_{IR}/L_B) against log (S_{100}/S_{60}). The outlined region shows the area occupied by normal spiral galaxies from Figure 2 of de Jong *et al.* (1984). Note that the ratios L_{IR}/L_B of de Jong *et al.* have been multiplied by 4.5 to put their L_B on the system used in this paper (see § II). The de Jong *et al.* L_B values were also corrected for internal absorption. For purposes of comparison, the Irr L_B values in this figure only have also been corrected for internal absorption in the same manner (Sandage and Tammann 1981), although this effect is small. One finds from Figure 3 that on average the Irr's have similar L_{IR}/L_B ratios compared with the spirals but warmer S_{100}/S_{60} dust color ratios (see also Deutsch and Willner 1986; Helou 1986). In a comparison with about 50 spirals chosen from Kennicutt's list, the median S_{100}/S_{60} for the spirals is 2.5, while for Irr's it is 1.5.

Figure 4 is a plot of the dust temperature-sensitive ratios S_{60}/S_{100} versus S_{12}/S_{25}. The outlined region shows the galaxies, largely spirals, plotted by Helou (1986) in his Figure 1. One can see from Figure 4 and from a comparison with data for Kennicutt's list of spirals that, in terms of the S_{25}/S_{12} ratio, the spirals are on average somewhat warmer than Irr's. Kennicutt's spiral sample has a median S_{25}/S_{12} of 1.5 compared with a median of 3 for our sample of Irr's. Thus, Irr's are warmer at 60 and 100 μm and cooler at 12 and 25 μm compared with spirals.

The Irr's also stand out as distinct from spiral galaxies in terms of the ratio $L_{IR}/L_{H\alpha}$. The $L_{H\alpha}$ values for spirals are taken from Kennicutt (1983) and are not corrected for internal extinction. The 48 spirals in this sample cover the same range as the Irr's (see Fig. 2), but the median value of $L_{IR}/L_{H\alpha}$ for the spirals is 150, while for the Irr's it is 70. This is consistent with the findings of Persson and Helou (1987) and Trinchieri,

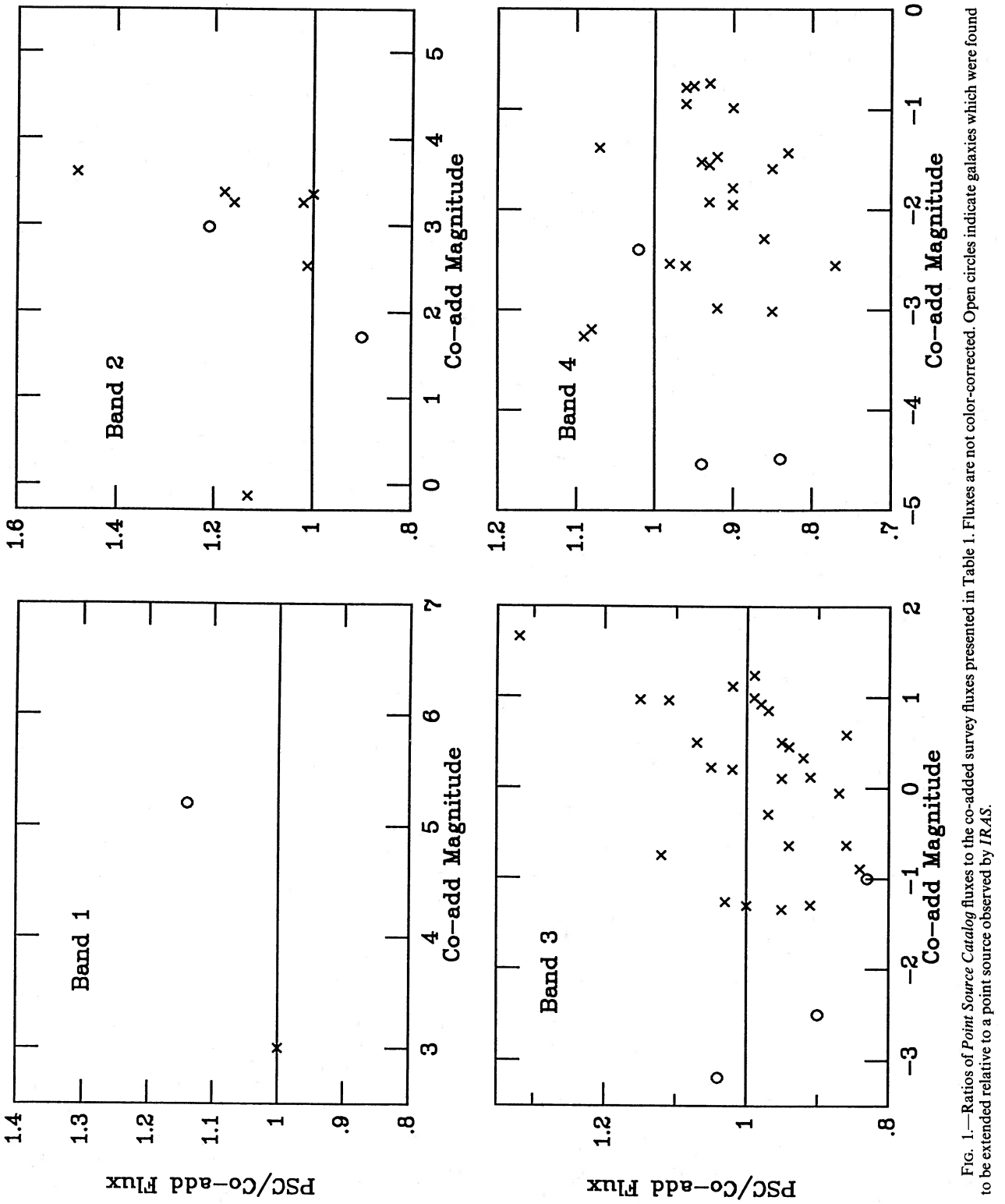

FIG. 1.—Ratios of *Point Source Catalog* fluxes to the co-added survey fluxes presented in Table 1. Fluxes are not color-corrected. Open circles indicate galaxies which were found to be extended relative to a point source observed by *IRAS*.

TABLE 3

INFRARED PROPERTIES OF IRREGULAR GALAXIES

Galaxy	S_{25}/S_{12}	S_{100}/S_{60}	$\log f_{IR}$	$\log L_{IR}$	L_{IR}/L_B	$L_{IR}/L_{H\alpha}$	T_D (K)	M_d	$10^4(M_d/M_{H\,I})$
Giants									
NGC 1012	1.19	1.57	−9.56	43.21	(4.4)	191	32	129	1.62
NGC 1156	3.00	1.67	−9.54	42.51	1.86	74	31	32	1.93
NGC 1569	9.72	1.12	−8.71	42.71	3.02	34	36	22	5.66
NGC 3274	...	1.71	−10.24	41.81	1.55	58	31	6.2	0.30
NGC 3510	...	2.60	−10.33	41.99	1.51	60	27	22.6	0.84
NGC 3738	...	1.74	−9.93	41.61	1.23	78	31	3.9	1.36
NGC 3952	...	1.34	−10.10	42.94	(2.9)	123	34	48.7	...
NGC 4214	4.97	1.81	−9.06	42.48	1.58	115	30	36.4	2.52
NGC 4449	2.18	1.98	−8.72	42.82	2.51	63	30	76	1.42
NGC 7292	...	1.95	−10.10	42.74	(1.5)	63	30	63	1.70
NGC 7800	...	2.09	−10.09	43.17	1.91	151	29	213	2.75
A1004+10	...	1.92	−10.47	41.41	(1.1)	33	30	3.0	...
Dwarfs									
DDO 42	...	1.06	−9.80	41.37	0.78	13	37	0.8	0.08
DDO 47	...	4.91	−10.91	40.23	0.46	525	23	1.1	0.63
DDO 49	...	1.72	−10.70	42.70	1.32	93	31	48.6	0.85
DDO 50	2.83	1.37	−10.00	41.16	0.44	27	34	0.8	0.07
DDO 53	...	1.74	−10.76	40.41	1.58	41	31	0.2	...
DDO 64	...	1.56	−10.89	41.15	1.12	91	32	1.1	0.28
DDO 75	1.09	...	...	...	...	...	...	...	...
DDO 140	...	1.65	−10.81	42.49	1.29	...	32	24.1	0.81
DDO 168	...	2.92	−10.74	40.82	0.34	...	26	2.0	0.89
DDO 218	...	2.09	−10.50	42.59	1.86	59	29	56.6	1.83
NGC 2552	...	1.99	−10.35	41.84	0.81	174	30	7.8	0.49
Amorphous									
NGC 1140	2.05	1.27	−9.78	43.26	3.16	69	34	106	1.43
NGC 1705	...	1.93	−10.22	41.74	1.02	30	30	6.3	...
NGC 1800	...	1.83	−10.27	41.97	1.20	78	30	11.2	3.23
NGC 4670	...	1.65	−9.81	42.93	3.80	49	32	66	...
NGC 5253	3.28	1.01	−8.93	42.82	3.89	51	38	20.8	4.15
Haro 22	...	...	...	...	...	...	...	...	...
Mrk 35	3.42	1.28	−9.60	43.10	7.41	110	34	73	6.21
II Zw 40	4.09	0.87	−9.59	42.78	20.4	24	40	15	1.93
Distant									
Mrk 314	...	1.05	−10.23	43.16	2.09	...	37	53	0.64
Mrk 390	...	1.63	−10.46	43.98	3.63	...	32	750	5.06
Haro 15	...	1.36	−10.15	44.15	2.69	...	34	790	6.3
Haro 20	...	1.62	−10.74	42.45	1.66	117	32	22.2	2.32
II Zw 23	1.58	1.43	−9.80	44.71	8.71	389	33	3460	8.90
II Zw 33	...	...	...	...	...	...	...	...	...
II Zw 185	...	...	...	...	...	...	...	...	...
III Zw 12	...	1.55	−10.28	43.96	7.08	282	32	730	10.8
III Zw 33	...	...	...	...	...	...	...	...	...
III Zw 42	1.64	1.56	−10.21	44.28	6.03	537	32	1530	42.1
III Zw 43	...	1.15	−9.90	43.88	8.13	...	36	316	13.8
IV Zw 149	4.08	1.33	−9.62	44.20	4.37	110	34	900	3.93

NOTE.—The flux f_{IR} is in units of ergs s^{-1} cm^{-2}. The luminosities are in units of ergs s^{-1}. Distances are taken from Kraan-Korteweg and Tammann 1979 or from radial velocities, and $H_0 = 50$ km s^{-1} Mpc^{-1}. Blue luminosities are taken from de Vaucouleurs, de Vaucouleurs, and Corwin 1976 (RC2); Gordon and Gottesman 1981; Kinman and Hintzen 1981; Hunter and Gallagher 1986. Values in parentheses are rough values from $m^c_{H\,I}$ (RC2) or estimated from magnitudes in Nilson 1973 (UGC) using the formulism of Corwin (private communication). Values of L_B are based on a solar blue magnitude of 5.41. Values of $L_{H\alpha}$ come from Hunter and Gallagher 1986. Galactic reddening corrections are taken from Burstein and Heiles 1984. The dust temperature T_D is calculated from $S_{60}/S_{100} = 4.63 \times 0.6^{-n}(e^{144/T} - 1)/(e^{240/T} - 1)$, where the spectral dependence of the dust-grain mass absorption coefficient is taken to be $n = 2$. M_d is the dust mass, in units of 10^4 $M_\odot$, for a silicate model using absorption efficiencies from Draine and Lee 1984 and the formalism of Gillett *et al.* 1986.

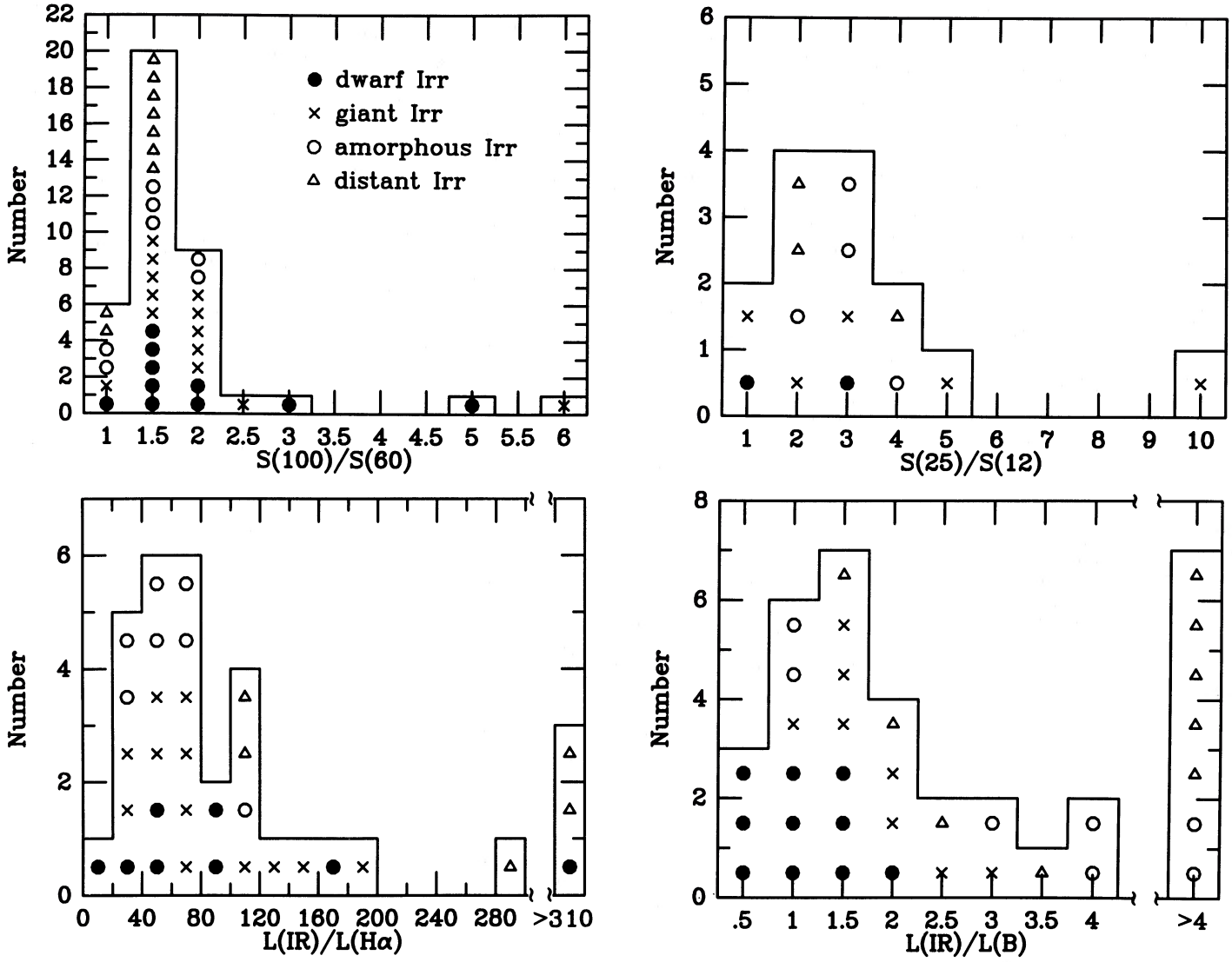

FIG. 2.—Number distribution of galaxies for various ratios of infrared and optical parameters. The Irr galaxies are grouped according to the classifications described in § I. The symbols distinguishing the different groups are used in all subsequent figures.

Fabbiano, and Bandiera (1989) that the infrared excess of galaxies decreases toward later Hubble type.

c) *Correlations with Optical Properties*

Figure 5 shows a plot of the infrared flux versus blue stellar flux, a measure of the general interstellar radiation field (GISRF), and versus the global Hα flux, a measure of the current star-formation activity, for Irr's and for spirals (see also Persson and Helou 1987; Trinchieri, Fabbiano, and Bandiera 1989). There is considerable scatter, but a trend can be seen in both plots. The solid lines are least-squares fits to the data. The correlation of f(Hα) with f(IR) is somewhat tighter than that of $f(B)$ with f(IR).

One might expect that the surface brightness of the radiation field would be important in governing the global dust properties such as temperature. In Figure 6 are plotted the dust temperature ratios S_{100}/S_{60} and S_{25}/S_{12} against the SFR per unit area of the galaxies. No significant correlation is seen. The optical surface brightness of a galaxy, on the other hand, is a measure of the GISRF per unit area, and it is plotted in Figure 7 against each of the temperature ratios. In Figure 7 there is a general trend for higher optical surface brightness to yield warmer S_{100}/S_{60} ratios. The two discrepant dwarfs in Figure 7 are DDO 42 and DDO 50, galaxies which are mainly dominated by a single giant H II region. A plot of optical surface brightness and SFR per unit area against L_{IR}/L_B in Figure 8 does suggest that galaxies with higher surface brightnesses, both stellar and Hα, have higher L_{IR}/L_B ratios.

d) *The Interstellar Medium*

Dust masses have been estimated using S_{60} and a silicate model, given by

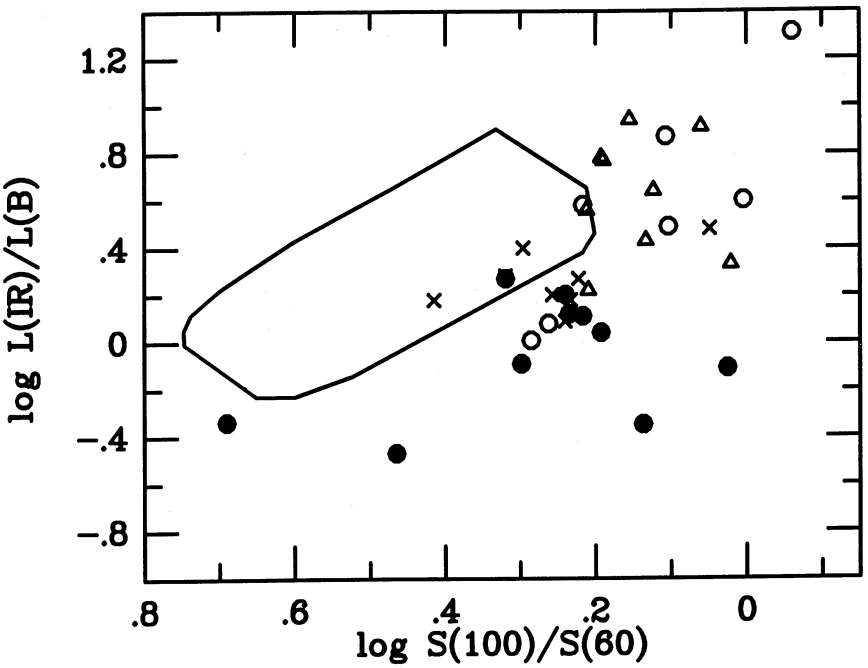

FIG. 3.—The log of the global infrared-to-blue luminosity ratio plotted against the log of the dust temperature-sensitive ratio S_{100}/S_{60}. The solid line outlines the region occupied by normal spiral galaxies as given in Fig. 2 of de Jong *et al.* (1984). The spiral L_B values have been multiplied by 4.5 to put them on the in-band flux system used in this paper. The L_B values of the Irr's have been corrected for internal absorption (Sandage and Tammann 1981). The different symbols denote different groups of Irr's as for Fig. 2.

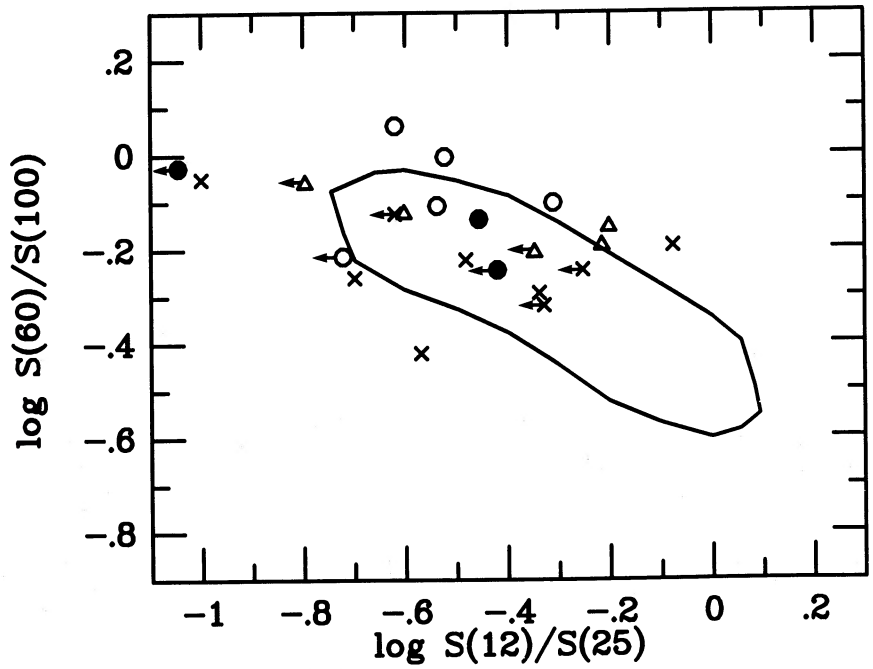

FIG. 4.—Log of the dust color-temperature–sensitive ratios S_{60}/S_{100} vs. S_{12}/S_{25}. The solid line outlines the region of normal galaxies plotted by Helou (1986) in his Fig. 1. Upper limits are shown with arrows for some objects. The different symbols are explained in Fig. 2.

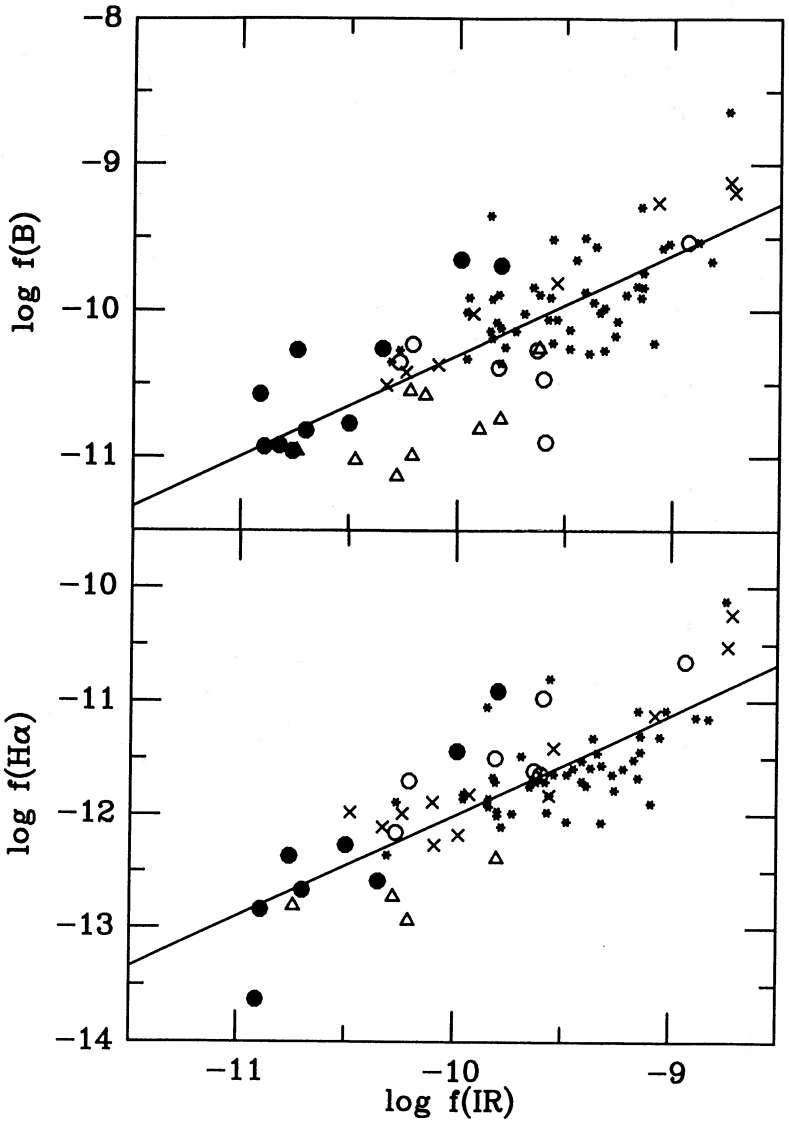

FIG. 5.—Infrared flux plotted against the global Hα flux and against the blue stellar flux for Irr's (symbols as in Fig. 2) and spirals (*small starred symbols*). Fluxes are used rather than luminosities because the distance-squared factor present in quantities along both axes can be misleading. The solid lines are least-squares fits to the data and are given by $\log f(\mathrm{H}\alpha) = 0.889[\log f(\mathrm{IR})] - 3.121$ and $\log f(B) = 0.688[\log f(\mathrm{IR})] - 3.425$.

$$M_d = 0.256 S_{60}(\mathrm{Jy}) D^2(\mathrm{Mpc})(e^{240/T_D} - 1) . \quad (1)$$

For graphite M_d would be approximately half of this. The temperatures, masses, and dust–to–H I gas mass ratios are given in Table 3. It is important to note that the dust and H I gas masses are global measurements rather than measurements of individual star-forming regions and that gas beyond the optical galaxy is not expected to contain dust that contributes to the *IRAS* infrared flux. Furthermore, there may be dust at cooler temperatures which does not contribute significantly to the *IRAS* passbands (cf. Chini *et al.* 1986; Thronson *et al.* 1987).

Finally, in spirals, a significant fraction of the interstellar gas is in the form of H_2. Typically $M(H_2)/M(\mathrm{H\ I}) \leq 1$; thus one could conservatively double the M(H I) for spirals to obtain an estimate for the total gas mass (cf. Bottinelli, Gouguenheim, and Paturel 1982; Young *et al.* 1986). The molecular gas content of Irr's is less certain but may be lower than that in spirals. Thus a comparison of $M_d/2M(\mathrm{H\ I})$ in spirals provides a fair zeroth-order approximation to the dust-to-gas ratio.

Keeping these points in mind, one can see from Figure 9 that for the dust measured by *IRAS* Irr's generally have lower global dust-to-gas ratios than spirals. This is contrary to the conclusion of Helou (1986). Studies (Werner *et al.* 1978; Viallefond, Goss, and Allen 1982; Viallefond, Donas, and Goss 1983; references in Koornneef 1984) of a few individual star-forming regions in the LMC suggest that *local* dust-to-gas ratios are also somewhat lower than comparable regions in spirals (see also Grieve and Madore 1986), although large optical depths due to dust can occur (Gatley *et al.* 1981).

Although the temperature-sensitive ratios S_{100}/S_{60} and S_{25}/S_{12} do not refer to a single temperature component of the

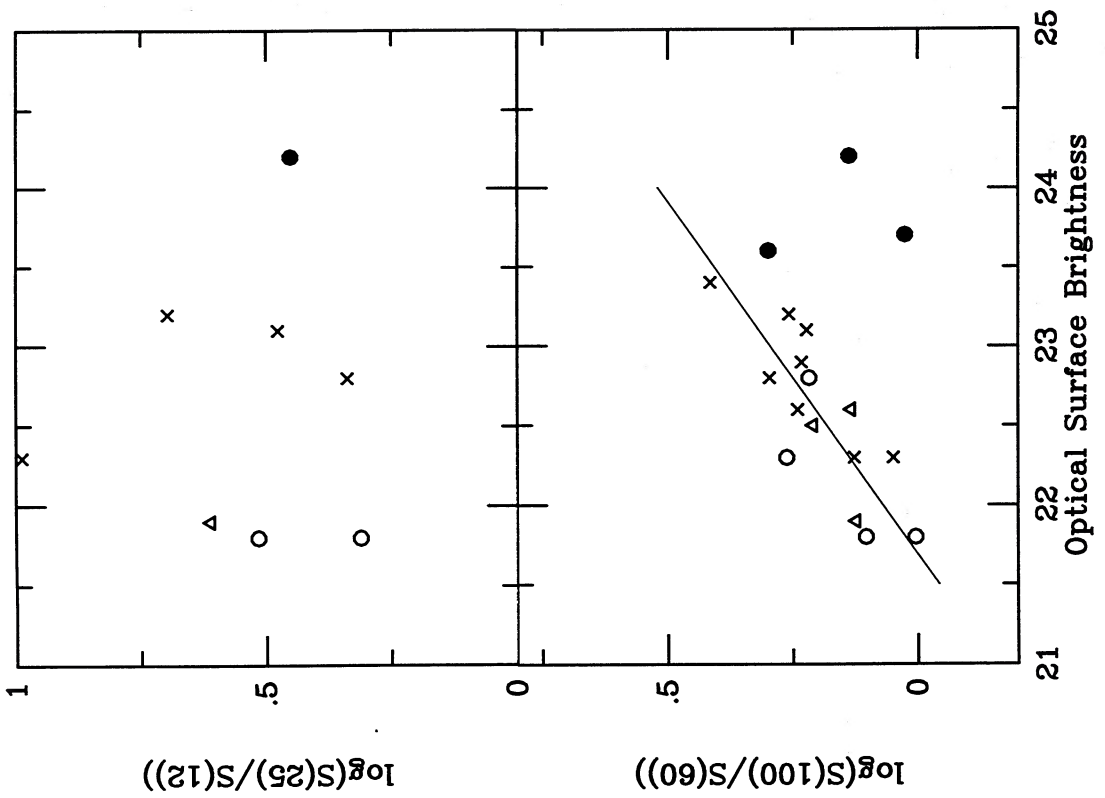

FIG. 7

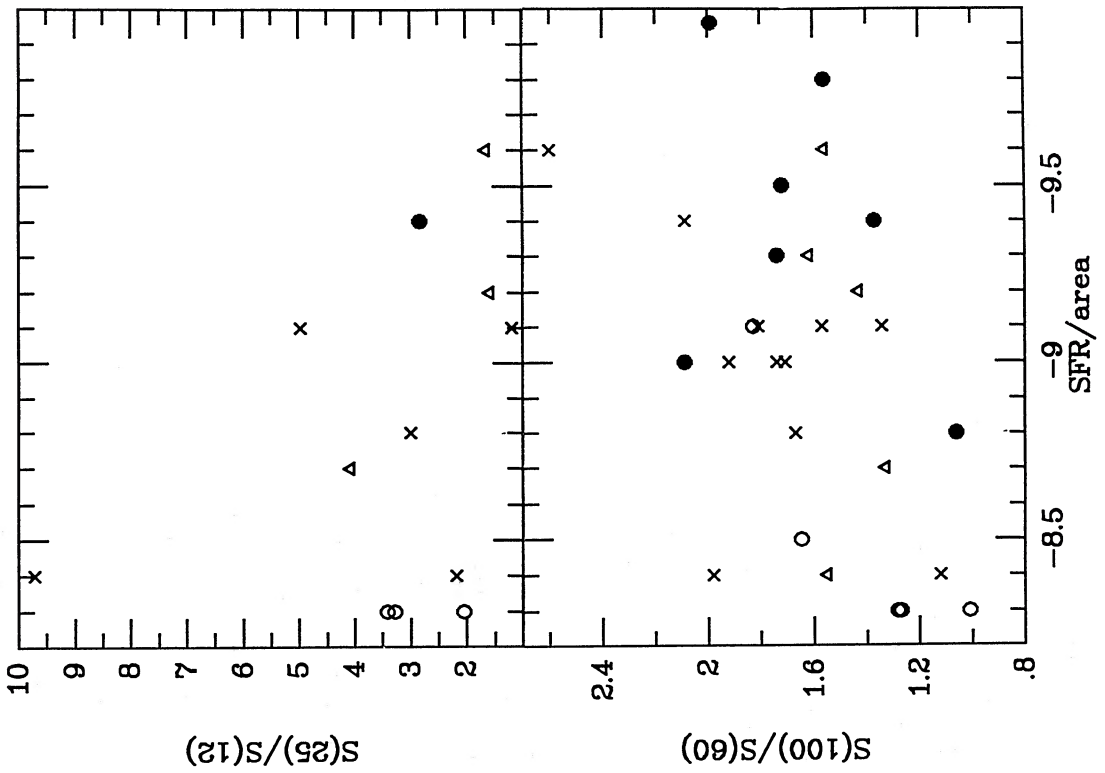

FIG. 6

FIG. 6.—Global SFR per unit area ($M_\odot$ yr^{-1} pc^{-2}) plotted against the temperature-sensitive ratios S_{100}/S_{60} and S_{25}/S_{12}. Symbols are explained in Fig. 2.
FIG. 7.—Blue optical surface brightness plotted against the log of the temperature-sensitive ratios S_{100}/S_{60} and S_{25}/S_{12}. The line is discussed in § V*b*. See Fig. 2 for an explanation of the symbols.

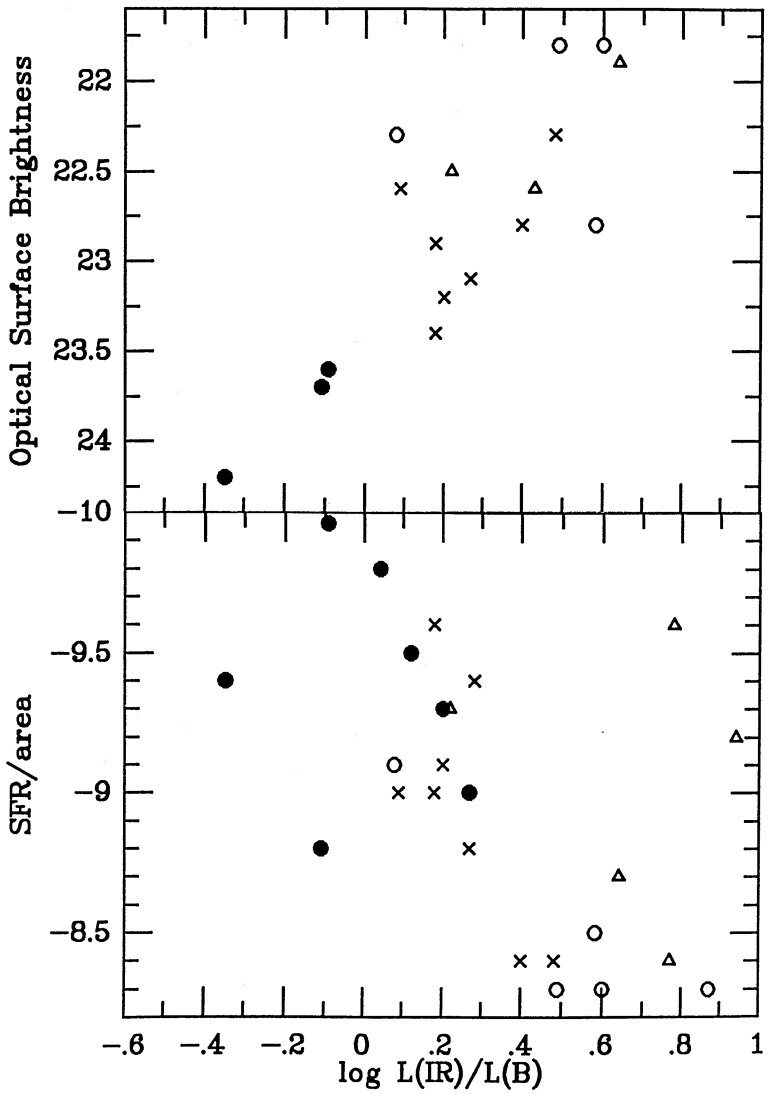

FIG. 8.—Infrared-to-blue luminosity ratio plotted against the SFR per unit area ($M_\odot$ yr^{-1} pc^{-2}), a measure of the intensity of the star-formation activity, and against the blue optical surface brightness, a measure of the GISRF. Symbols are explained in Fig. 2.

dust, these ratios do give an idea of the average temperature of the dust contributing to those passbands. One can then ask why these temperature-sensitive ratios vary from Irr to Irr. Figure 10 shows that there is no trend of the S_{100}/S_{60} temperature ratio with absolute luminosity of the Irr.

One explanation for temperature variations comes from Thronson and Mozurkewich (1989). They found that the Milky Way star-forming regions cover the S_{60}/S_{100} versus S_{12}/S_{25} plane and concluded that variations in the relative numbers of high- and low-temperature star-forming regions or the molecular cloud mass function result in temperature variations among galaxies (see also de Muizon and Rouan 1985). Of course, this does not explain why there would be differences in the molecular cloud mass functions among galaxies, especially among galaxies with otherwise very similar optical properties and stellar population characteristics. In a study of LMC H II regions Werner *et al.* (1978) suggest that lower dust temperatures in the LMC compared with the Milky Way are due to the lower dust density in the LMC star-forming regions.

One factor which can affect the dust temperature is the composition of the dust grains; everything else being the same, graphite grains will be warmer than silicate. One might expect that, if composition of the grains is the dominant factor affecting the overall temperature variation in the dust between galaxies, the temperature ratios S_{100}/S_{60} and S_{25}/S_{12} would be correlated with the metallicity of the galaxies. Spiral galaxies are in general more metal-rich than Irr's, and there are temperature differences as noted in § III*b*. The quantity ([O II] + [O III])/Hβ, measured from emission lines in H II regions, is sensitive to the abundance of the ionized gas (Pagel *et al.* 1979), so we use it here as an indicator of the metallicity of a galaxy (Hunter, Gallagher, and Rautenkranz 1982; Hunter and Gallagher 1985*a*, 1986; Gallagher, Hunter, and Bushouse 1989; see these references also for a discussion of com-

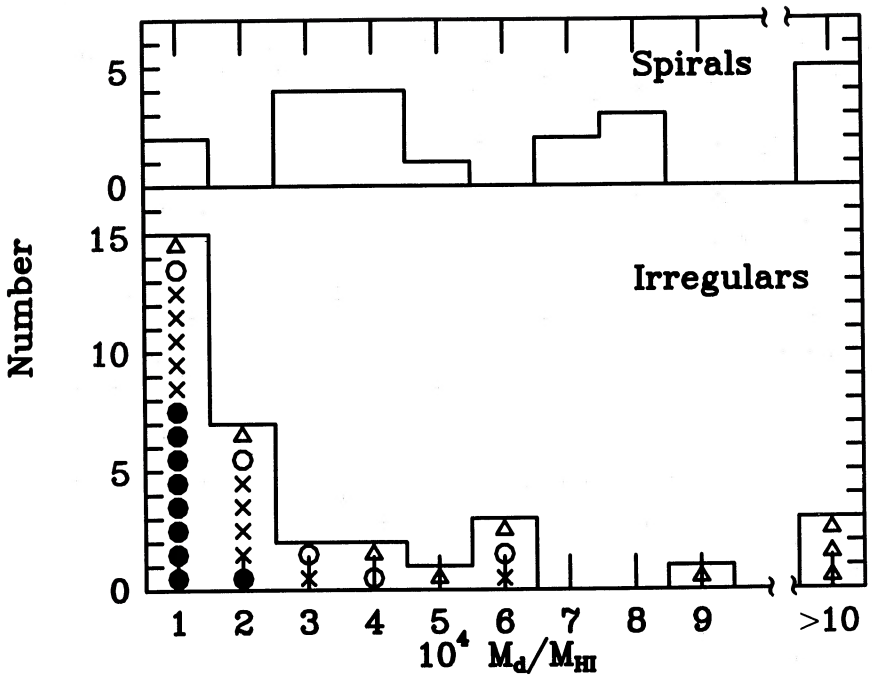

FIG. 9.—Number distribution of global dust–to–H I gas mass ratios for irregulars and spirals. The spirals were chosen from Kennicutt's (1983) list, and their H I measurements come from Fisher and Tully (1981). Irregular galaxy symbols are as in Fig. 2.

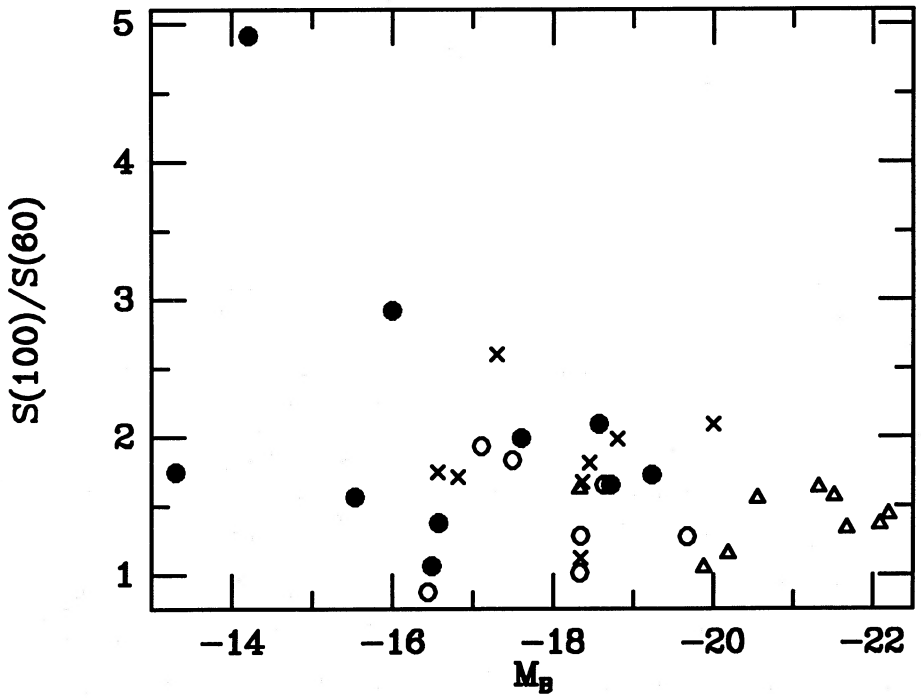

FIG. 10.—Absolute blue luminosity vs. dust temperature ratio S_{100}/S_{60}. Symbols are defined in Fig. 2.

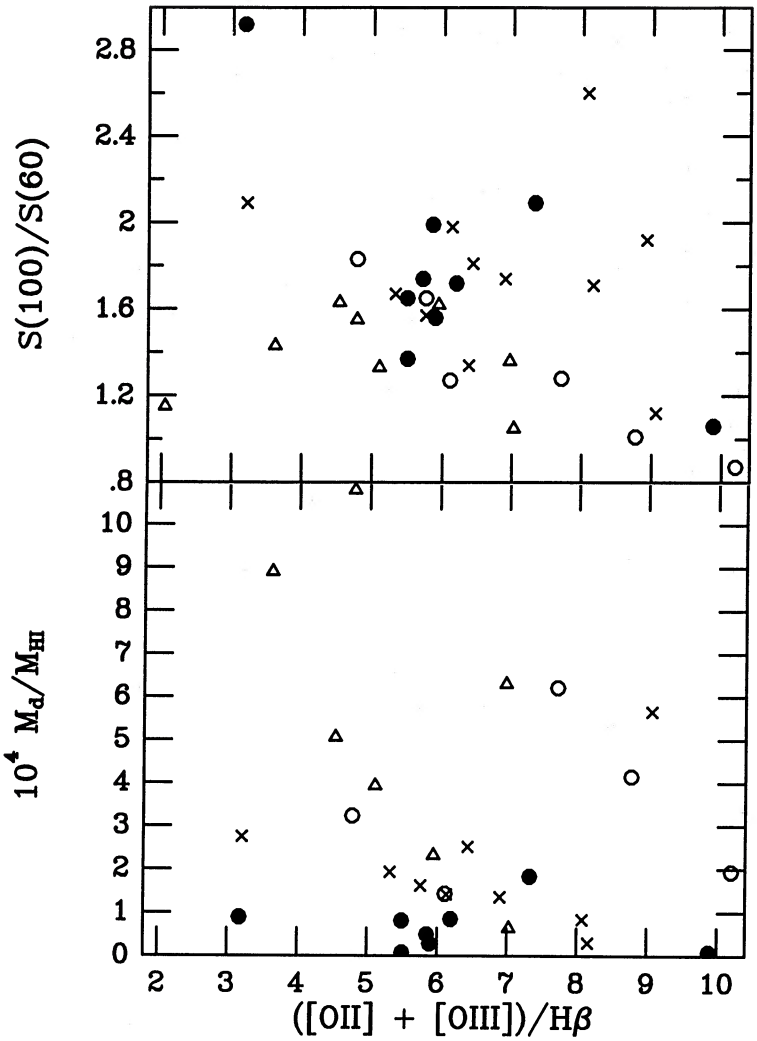

FIG. 11.—Metallicity-sensitive ratio ([O II] + [O III])/Hβ, determined from gaseous emission lines, plotted against the temperature ratio S_{100}/S_{60} and the dust-to-H I gas mass ratio. Symbols are defined in Fig. 2.

plications). In Figure 11 is plotted S_{100}/S_{60} against the ratio ([O II] + [O III])/Hβ. Among the Irr's, at least, no correlation is seen. Furthermore, there is no correlation of the dust–to–H I gas ratio with metallicity. Figure 12 is a plot of L_{IR}/L_B against ([O II] + [O III])/Hβ and M_d/M_{HI}. Again, no correlations are seen. Therefore, the effect of the metallicity on the dust is not obvious or simple, and interpretation of the temperature variation will be more complex.

Another factor which can be very important, especially at shorter infrared wavelengths, is the presence of small grains. The recent study of the California Nebula by Boulanger *et al.* (1988), for example, suggests that nonequilibrium heating of small grains has a major effect on the values of S_{12}/S_{25} and S_{25}/S_{60}. They also point out that small grains are likely to be destroyed in high-radiation field energy density environments, and there may also be unknown abundance-dependent effects on the production ratios of small to large grains in different types of galaxies.

IV. SOURCES OF DUST HEATING AND MODELS

Traditionally it has been thought that radiation from stars in star-forming regions is responsible for heating the dust in the *IRAS* passbands. Models by de Muizon and Rouan (1985) show that for 20–150 μm OB stars are more effective than the GISRF in heating the dust. But with *IRAS* it has been found that infrared cirrus can be a significant contribution to a galaxy's total FIR flux (Persson and Helou 1987), and it has been suggested that it could be the dominant contribution (Helou 1986). The nature of the "cirrus" is not entirely known yet, but it could result from small grains heated by the GISRF and hence be disconnected from the current star-forming activity. Walterbos and Schwering (1987), for example, conclude that in M31 only 10% of the infrared radiation comes *directly* from regions of star-forming activity. The problem in dealing with the *IRAS* integrated fluxes of galaxies is in determining the relative contributions of these two, as well as other sources (cf. Thronson and Bally 1987; Boulanger *et al.* 1988;

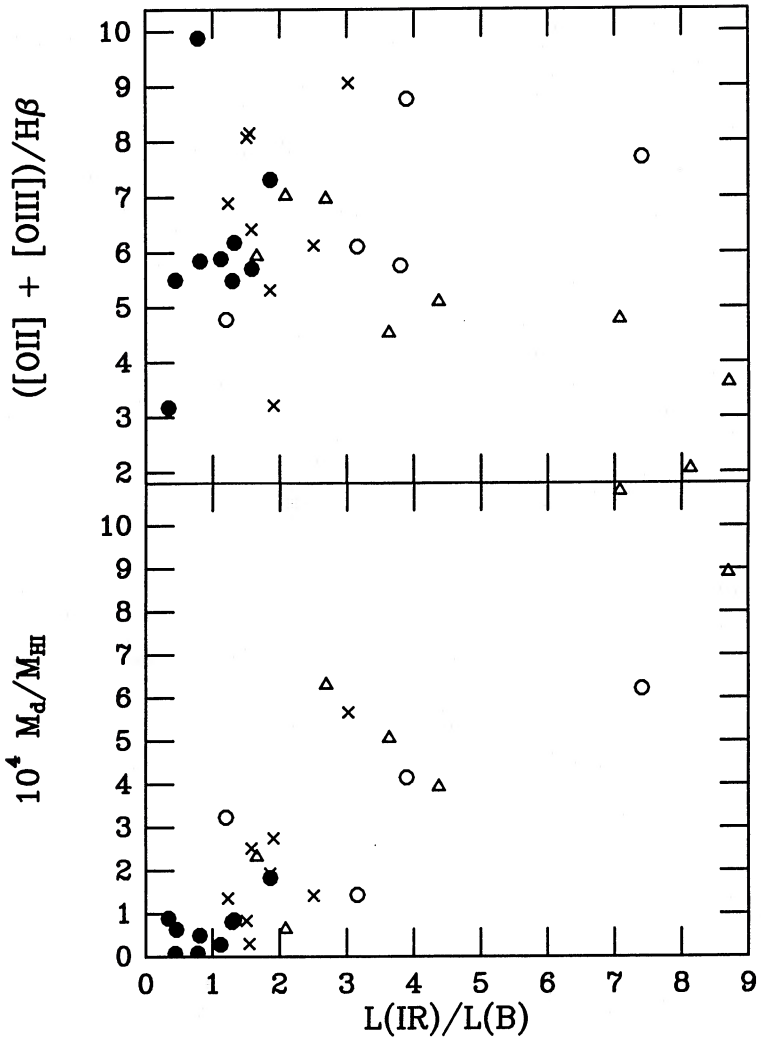

FIG. 12.—L_{IR}/L_B plotted against the global dust–to–H I gas mass ratio and the metallicity-sensitive ratio ([O II] + [O III])/Hβ. See Fig. 2 for symbol definitions.

Trinchieri, Fabbiano, and Bandiera 1989).

However, there are some indications that the *IRAS* radiation *is* connected with the star-formation activity, at least in some cases. First, one aspect of the infrared cirrus is that it is cold. S_{100}/S_{60} color ratios are ~3–7 (Low *et al.* 1984). In M31, where the GISRF has been shown to dominate, this ratio is ~5. In Figure 3 we saw that spiral galaxies in general have higher S_{100}/S_{60} ratios than irregulars. One explanation of this difference is that irregulars contain a much smaller component of cirrus; i.e., the dominant source of heating of the dust is star formation, whereas in spirals the dominant source is the GISRF (Persson and Helou 1987). Second, Haslam and Osborne (1987) have compared 60 μm maps of the Milky Way with 11 cm maps and found that the 60 μm flux is very well correlated with extended low-density H II regions. Mezger, Mathis, and Panagia (1982) have further suggested that the diffuse FIR and submillimeter radiation arises from these extended low-density H II regions and diffuse H I gas. They conclude that the FIR emission is connected, directly or indirectly, to OB star formation. Third, partially resolved *IRAS* maps of NGC 4449 at 12 and 25 μm suggest a correlation with locations of OB star formation (Hunter *et al.* 1986). Fourth, models such as those by Boulanger *et al.* (1988) show that small grains have little effect on S_{100}/S_{60} ratios in the range observed for irregular galaxies. Thus, there is some indication that the *IRAS* radiation is associated with star formation to a significant degree in Irr's (cf. Telesco and Harper 1980).

There is a considerable complication, however, that arises in trying to separate the star-formation and non–star-formation components of the heating from global properties. For example, in constant SFR systems such as the Irr's, the GISRF is a function of the current star-formation activity (cf. Hunter and Gallagher 1986; Thronson and Telesco 1986). Thus, the two sources of radiation are themselves correlated. In an attempt to deconvolve the sources of radiation, we present below simple models which we compare with the observations in § V.

a) Basic Concepts

The difficulty in deducing the specifics of the stellar dust-heating processes that yield L_{IR} in galaxies from global measurements stems from the fact that L_{IR} depends on global

integrals over *local* galactic properties,

$$L_{\rm IR} = 4\pi c D^2 E \int_V \int_\lambda U_*(\lambda, r)\bar{\sigma}_D(\lambda)\rho_D(r)d\lambda\, dr\ . \qquad (2)$$

Here c is the speed of light, E is a coupling efficiency between the total power radiated by dust grains and that included in the *IRAS*-based measurement of $L_{\rm IR}$, U_* is the stellar radiation field energy density, $\bar{\sigma}_D$ is the average grain absorption cross section, and ρ_D is the local dust density (e.g., Mezger, Mathis, and Panagia 1982). The relationship between $L_{\rm IR}$ and the local parameters in equation (2) are further complicated by the fact that U_* is itself dependent on an integral over galactic structural properties and is sensitive to the specifics of the distributions of both dust and stars (Mathis 1973; Mathis, Mezger, and Panagia 1983).

The second observable FIR characteristic of galaxies, the FIR spectral energy distribution, depends on U_* and on dust characteristics (e.g., grain sizes and compositions). For a standard interstellar particle of fixed size, one expects $T_D \approx AU_*^{1/5}$, which leads to a natural association between hot dust and high U_* environments (such as H II regions), while cold dust is relegated to heating by the low-energy density GISRF. Unfortunately, the existence of warm FIR color-temperature emission in the short-wavelength *IRAS* bands from high Galactic latitude cirrus clouds establishes that grain-related parameters can also play an important role in modifying the FIR spectra of galaxies (cf. Low *et al.* 1984; Helou 1986; Rowan-Robinson 1986; Soifer, Houck, and Neugebauer 1987; Boulanger *et al.* 1988).

In our discussion of FIR properties of optically blue irregular galaxies, we will therefore rely on only the most general classes of models. Following the approach described by de Jong and Brink (1987), we consider the stellar population to consist of only two age components, with index 1 referring to stars with ages $< 10^8$ yr and 2 for stars with ages $\geq 10^8$ yr. If $\bar{\tau}'_B$ is a galactic mean *absorption* optical depth, then the observed L_B is

$$L_B = [L_B^0(1) + L_B^0(2)] \exp(-\bar{\tau}'_B)\ . \qquad (3)$$

When young stars are important contributors to the total bolometric stellar luminosity, as in Irr galaxies, then most of the stellar power is radiated in the UV. We then have $L_{\rm UV}^0 = R_{\rm UV} L_B^0(1)$ with a proportionality constant $R_{\rm UV} > 1$. Furthermore, since absorption optical depths scale approximately as $\bar{\tau}'_{\rm UV}(\lambda) = \bar{\tau}'_B \lambda^{-n}$, $n \approx 1$, the UV stellar radiation field will strongly couple to the dust and will dominate dust heating in blue galaxies.

As discussed by Cox, Krügel, and Mezger (1986), only dust in the immediate vicinity of stars has been observed to have warm or hot S_{100}/S_{60} color temperatures. Conversely, due to the effects of FIR cirrus, *any* color-temperature component of galactic *IRAS* $L_{\rm IR}$ can contain substantial contributions from young stars (see also Lonsdale, Rice, and Bothun 1987; Thronson and Mozurkewich 1989). A local example is provided by IR cirrus in the Pleiades, where the cirrus is clearly heated by young B stars (Cox and Leene 1987). Another example is M33, which is a UV-bright galaxy (Code and Welch 1982; Israel, de Boer, and Bosma 1986) containing a large Population I stellar component and diffuse ionized gas, with FIR color characteristics of a cirrus-dominated galaxy (Helou 1986). Similarly, Boulanger and Pérault (1988) conclude that most of the solar neighborhood $L_{\rm IR}$ is provided by young stars, even though much of the dust responsible for $L_{\rm IR}$ lies outside star-forming regions. Arguments based *solely* on the use of global FIR colors to separate dust-heating contributions from young and old stellar populations can therefore be misleading in systems with substantial Population I components in the sense that radiation from young stars can produce cool IR color temperatures at long wavelengths (cf. Helou 1986; de Jong and Brink 1987).

In blue galaxies it is therefore likely that all wavelength components of the *IRAS* $L_{\rm IR}$ contain substantial contributions from heating by young stars. In §§ IV*b* and IV*c* we consider the role of younger stars in producing $L_{\rm IR}$ in Irr's via a two-component model consisting of discrete H II region sources and a UV-dominated GISRF. In this discussion we emphasize the S_{100}/S_{60} ratio, as it is least dependent on nonequilibrium radiation from small grains and thus is most sensitive to local radiation-field characteristics.

b) Far-Infrared Luminosity from H II *Regions*

Contributions to $L_{\rm IR}$ by H II regions can be distinguished by their correlation with other characteristic H II region emissions, such as $L_{\rm H\alpha}$ or thermal radio luminosity. Since Irr's often have low-absorption optical depths at visible wavelengths, $L_{\rm H\alpha}$ is a particularly powerful probe of H II region content in these galaxies. The expected ratio of $L_{\rm IR}/L_{\rm H\alpha}$ can then be approximately predicted from simple theoretical models.

The Lyman continuum power responsible for producing $L_0(\rm H\alpha)$ from an H II region is

$$L(\rm Lyc) = 16(\overline{h\nu}/13.6\ \rm eV)\eta^{-1} L_0(H\alpha)\ , \qquad (4)$$

where $L_0(\rm H\alpha)$ is a total luminosity corrected for extinction in and around the H II region, η^{-1} is an efficiency factor, and $\overline{h\nu}$ is the average Lyman continuum photon energy, which depends on the temperatures of the ionizing stars. The total stellar luminosity of the H II complex is then

$$L(\rm bol) = uL(Lyc)\ , \qquad (5)$$

with $u > 1$ as a result of substantial power contributions by OB stars at $\lambda > 912$ Å. For example, in the giant LMC H II region 30 Doradus, $u \geq 2$ (Werner *et al.* 1978; Israel and Koornneef 1979). Finally, a fraction f of L(bol) is absorbed by dust to produce $L_{\rm IR}$,

$$L_{\rm IR} \sim uf16(\overline{h\nu}/13.6\ \rm eV)\eta^{-1} L_0(H\alpha)\ . \qquad (6)$$

In a typical case we observe

$$L_{\rm H\alpha} = L_0(\rm H\alpha) \exp[-\overline{\tau_a(H\alpha)}]\ , \qquad (7)$$

where $\overline{\tau_a(\rm H\alpha)}$ is an average over the galaxy of the absorption optical depth at Hα. The diagnostic ratio of observable luminosity thus is

$$L_{\rm H\alpha} = \frac{L_{\rm IR}}{uf\eta^{-1}16(\overline{h\nu}/13.6\ \rm eV)\exp[\overline{\tau_a(H\alpha)}]}\ . \qquad (8)$$

As an example, we consider the $L_{\rm H\alpha}/L_{\rm IR}$ ratio expected if OB stars produce all of $L_{\rm IR}$ in a typical Im system. As a preliminary calibration, the Magellanic Cloud FIR data of Werner *et al.* (1978) suggest $uf\eta^{-1} \gtrsim 1$ and $\tau_a(\rm H\alpha) \sim 0.2$ [$E(B-V) \sim 0.3$]. The H II region component of a galaxy will then produce

$$L_{\rm IR} \sim (10 - 30)L_{\rm H\alpha} \qquad (9)$$

on the basis of our simple model.

A second, but somewhat uncertain, FIR signature of large ($L_{IR} \gtrsim 10^6\ L_\odot$) H II complexes is warm S_{100}/S_{60} dust temperatures. For example, Scoville and Good (1987) found $T_D \sim$ 35–40 K for several Galactic H II regions observed by *IRAS*. The more extensive tabulation of Galactic H II region *IRAS* observations by Thronson and Mozurkewich (1989) shows a similar range of T_D for luminous H II regions, although many lower luminosity H II regions are cooler; so unique matches between T_D and environment remain problematical. Magellanic Cloud H II region observations by Werner *et al.* (1978) and Eastwood (1989) similarly suggest that $T_D \sim 30$–40 K ($S_{100}/S_{60} \sim 1.5$) is typical.

In order to make further progress, we will now assume that high T_D values derived from galactic *IRAS* S_{100}/S_{60} ratios are good indicators of large contributions to L_{IR} from H II regions. This correlation is also the basis of the de Jong and Brink (1987) method for separating the young population contribution to L_{IR} from galaxies. The full range of *IRAS* colors cannot be used to separate temperature components, since short-wavelength FIR emission may be heavily contaminated by high color temperature emission from cirrus, which is located well away from H II regions. In analyzing *IRAS* observations of Irr's, we will combine information on T_D based on S_{100}/S_{60} with $L_{IR}/L_{H\alpha}$ to estimate L_{IR} contributions by very young stars in H II regions (ages $\leq 10^7$ yr).

c) *The GISRF*

A dust grain in an arbitrary location in the disk of an Irr galaxy will be heated by the GISRF. From equation (2) the amount and color temperature of L_{IR} from this dust component depend on a complex combination of factors, including the spectrum and energy density of the GISRF. Figure 13 shows the emergent optical-UV-infrared spectrum from the giant galaxy NGC 4449, which includes almost all of the stellar-powered flux. This spectrum should be representative of many of the galaxies in our sample, most of which have not been observed in the UV.

Most of the stellar luminosity in blue irregular galaxies is radiated over 912–2000 Å, with a secondary peak in the visual from evolved descendants of longer-lived stars (see Fig. 13). The UV spectral energy distributions resemble mid to late B spectral class stars (Wesselius *et al.* 1982; Lamb *et al.* 1985). Although these energy distributions result from a combination of stellar temperature classes, the blueness of the UV colors suggests that the UV GISRF will be dominated by stars with lifetimes of $\leq 3 \times 10^8$ yr (Lamb, Hunter, and Gallagher 1989). Figure 13 also shows that λf_λ is *not* a useful indicator of total stellar luminosities when applied to optical fluxes from Irr galaxies.

The detailed properties of the GISRF within galactic disks are not easily predictable, because of uncertainties in UV grain and stellar-population characteristics. We therefore consider how the GISRF as given by U_* would depend on properties of two classes of idealized galactic disk models. In a fully transparent disk, U_* will depend on the luminosity density and structure of the stellar disk. For example, $U_*(\lambda, 0)$ at the center of a thin disk with luminosity surface density $l_0(\lambda)$ and radius D is

$$U_*(\lambda, 0) \approx \frac{2\pi l_0(\lambda) \ln (D)}{c} . \quad (10)$$

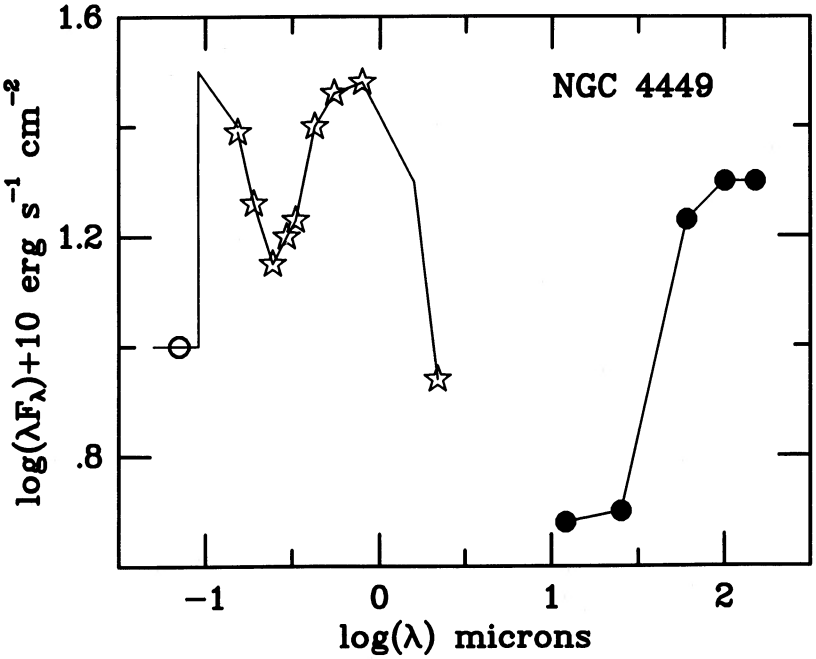

FIG. 13.—This plot shows the stellar and thermal dust emission from integrated photometric observations of the Im III galaxy NGC 4449. The Lyman continuum point (*open circle*) is based on Hα flux measurements (Gallagher, Hunter, and Tutukov 1984); UV data are *OAO* photometry from Code and Welch (1982); the *V*-magnitude is from the RC2 (de Vaucouleurs, de Vaucouleurs, and Corwin 1976); the *I*-band point assumes $V-I = 0.7$ (Hunter, Gallagher, and Rautenkranz 1982); and the *K* point assumes $V-K = 2.0$ (Hunter and Gallagher 1985*c*). The stars and Lyman continuum points cover most of the direct radiation by stars. The IR data are *IRAS* observations plus a KAO 150 μm point from Thronson *et al.* (1987). Note that λF_λ at optical wavelengths is *not* a good indicator of stellar bolometric luminosity.

At the other extreme, U_* in an optically thick galactic disk depends primarily on the local stellar luminosity source function,

$$S_*(\lambda) = \epsilon_*(\lambda)\rho_* k_d^{-1}(\lambda) = \frac{C\epsilon_*(\lambda)\rho_*}{\rho_{\rm gas}} . \quad (11)$$

Here $\rho_* \epsilon_*$ is the stellar emissivity (ergs s^{-1} $Å^{-1}$ sr^{-1} cm^{-3}), and k_d is the dust absorption coefficient (cm^{-1}; see Jura 1980). In this case

$$U_*(r, \lambda) \approx S_*(r, \lambda)[1 - \exp(-\tau_\lambda)]\Omega(\text{disk})c^{-1} , \quad (12)$$

where Ω(disk) is the solid angle of the optically thick stellar disk as viewed from a position at r within the disk.

Real gassy galactic disks will lie between these two extremes. In the UV, where optical depths will almost always be large, equation (12) would apply in an idealized uniform galaxy. However, since the interstellar medium (ISM) is not uniformly distributed in Irr galaxies, on average there is also likely to be a significant contribution to U_* from distant parts of the galaxy seen through low-density holes in the cool ISM. Another complication is the presence of diffuse, ionized gas in many Irr's, which indicates that Lyc photons should also be considered to be part of the GISRF (Hunter 1984; Hunter and Gallagher 1986). Yet in all cases the crucial UV GISRF will increase with stellar Population I surface densities and thus with UV surface brightness.

The limited data available on the UV surface brightnesses of Irr's for $\lambda \leq 2000$ Å suggest that these types of galaxies do have higher UV-to-optical surface brightness ratios than spirals (e.g., Coleman, Wu, and Weedman 1980; Maucherat-Joubert, Lequeux, and Rocca-Volmerange 1980; Israel, de Boer, and Bosma 1986). For example, the giant Im galaxy NGC 4449 has higher UV surface brightness in the inner 2.5 than comparable regions of spirals. The high UV surface brightnesses of Im systems also extend to the nearly edge-on galaxy NGC 55 (Code and Welch 1982; Carruthers and Page 1983). Thus we conclude that average interstellar grains in at least Im Irr's are bathed in a bluer and more intense GISRF than average grains in spiral galaxies of comparable optical surface brightness. If grain characteristics were similar in spirals and Im galaxies, then the diffuse FIR emission would have warmer S_{100}/S_{60} color temperatures in Im galaxies, which is what is observed (see § III*b*).

While the origins of the high UV surface brightnesses and high U_* in Im galaxies to our knowledge have not been formally discussed in the literature, it is likely that enhanced S_*(UV) results in part from decreased dust opacities, at least in Magellanic and amorphous Irr's (see § III*b*). The absorption optical depths in Im galaxies would then be systematically lower than in spirals, and OB starlight could more readily escape, leading to higher UV surface brightnesses. These effects are further enhanced by the likely presence of large holes in the cool ISM in Irr galaxies (cf. the discussion of LMC Constellation III by Meaburn 1980). It is less likely that Irr galaxies have higher densities of OB stars than spirals, since mean Hα surface brightnesses are similar in these two classes of galaxies (Hunter and Gallagher 1986). As a result of the increased escape efficiency for UV photons, a smaller fraction of $L^0_{\rm UV}$ will be converted into $L_{\rm IR}$. The signature of reduced absorption of OB stellar luminosity in Im galaxies is then the presence of warm, diffuse FIR emission in combination with a decreased $L_{\rm IR}/L$(stellar) ratio from the diffuse FIR component relative to these parameters in spirals.

V. ORIGINS OF FAR-INFRARED EMISSION IN IRREGULAR GALAXIES

a) H II *Region–dominated Systems*

Far-infrared radiation is produced primarily in or near H II regions in two classes of galaxies: (1) Some galaxies, such as II Zw 40, are powered by extreme Population I stars at all wavelengths from the UV to the FIR. We will label these as type 1 H II galaxies. (2) In type 2 H II galaxies, $L_{\rm IR}$ and $L_{\rm H\alpha}$ are both produced by H II regions, but luminosity at L_B and other wavelengths includes substantial contributions from more spatially extended, older stellar population components, i.e., the $L^0_B(2)$ term in equation (3) is important. We discuss a third option, where both L_B and $L_{\rm IR}$ are powered by a range of stellar ages, under the heading of complex galaxies in § V*b*.

Type 1 H II galaxies are readily identified in the optical by their blue continua due to Population I stars and nebular continuum emission in combination with pronounced nebular emission lines. To qualify as a type 1 H II galaxy, we require either (1) that the Hα emission-line width integrated over the optical dimensions of the galaxy exceed 100 Å (or that the pseudo–equivalent width $L_{\rm H\alpha}/L_B \gtrsim 0.1$; Gallagher and Hunter 1987*a*) or (2) that the global Hα emission equivalent width be $\gtrsim 60$ Å ($L_{\rm H\alpha}/L_B \gtrsim 0.05$) and that the Hα emission extend over dimensions comparable to the stellar galaxy in most locations (e.g., NGC 1569; Hodge 1974; Hunter 1982). These criteria are designed to select galaxies whose integrated optical properties resemble those of 30 Doradus–type giant H II regions which have $L_{\rm H\alpha}/L_B \gtrsim 0.1$ and larger Hα than stellar dimensions (see Hunter and Gallagher 1985*a*). II Zw 40 meets both criteria and is essentially a supergiant H II region which is its own galaxy.

By this definition, our sample of Irr's includes six type 1 H II galaxies which are listed along with basic properties in Table 4. Most of these are amorphous galaxies, which as a class show evidence for unusual spatial distributions of star-forming regions and consequently unusual evolutionary histories (Gallagher and Hunter 1987*b*).

The mean FIR characteristics of the type 1 H II galaxies in

TABLE 4

TYPE 1 H II GALAXIES

Galaxy	Type	M_B	$D_{\rm H}$ (kpc)	$L_{\rm H\alpha}/L_B$	H II Distribution
NGC 1140	Amorphous	−19.7	22	0.046	Central complex
NGC 1569	Im III:	−18.4	19	0.089	Extended
NGC 4670	Amorphous	−18.6	21	0.078	Central complex
NGC 5253	Amorphous	−18.3	15	0.076	Central complex
Mrk 35	Amorphous	−18.4	15	0.067	Extended
II Zw 40	Amorphous/H II	−16.4	24	0.85	Extended

Table 4 can be summarized as $\overline{L_{IR}/L_{H\alpha}} = 56 \pm 14$ and $S_{100}/S_{60} = 1.2 \pm 0.1$, which are near the values adopted for galactic H II regions in § IV*b*. The slightly high value of $L_{IR}/L_{H\alpha}$ as compared with equation (9) probably is caused by the presence of evolved OB supergiants which contribute substantially to L_{UV} and $L_B^0(1)$ in these galaxies. The supergiants are likely to be produced from stars that formed *before* the current generation of main-sequence OB stars responsible for nebular ionization (i.e., $u > 2$ in eq. [5]). NGC 1569 stands out from H II regions because of its steep short-wavelength infrared spectrum, $S_{25}/S_{12} = 9.7$; but the other three type 1 galaxies have normal LMC H II region colors of $S_{25}/S_{12} = 3$–4 (e.g., Eastwood 1989). The combination of galactic H II region–like infrared properties and energetics arguments reviewed in § IV*b* shows that FIR characteristics of type 1 H II galaxies reflect an overall dominance of extreme population I stars (see also Joy and Lester 1988).

For galaxies with low optical absorption levels, we then expect that systems in which L_{IR} is causally associated with H II regions will have $S_{100}/S_{60} \leq 1.5$ (cf. de Jong and Brink 1987) and $L_{IR}/L_{H\alpha} \leq 70$. This model does not apply to many of the distant irregulars, because they may be optically thick at visible wavelengths, and we discuss these galaxies separately below.

Of the remaining galaxies in Table 3, DDO 42, DDO 50, and possibly DDO 53 are Type 2 H II galaxies. NGC 3952 satisfies the S_{100}/S_{60} condition for H II region–dominated galaxies, but has excessively high $L_{IR}/L_{H\alpha}$. This could be due to high internal extinction toward H II regions in this nearly edge-on galaxy, which is consistent with the $E(B-V) = 0.8$ measured toward one NGC 3952 H II region by Hunter, Gallagher, and Rautenkranz (1982). DDO 42 (NGC 2363), DDO 50 (Holmberg II), and DDO 53 all contain a dominant H II complex which is large relative to their low surface brightness stellar bodies (cf. Hunter and Gallagher 1985*b*). Furthermore, DDO 42 and DDO 50 have low L_{IR}/L_B ratios as expected if L_{IR} is not closely tied to L_B, i.e., L_B is dominated by the $L_B^0(2)$ term in equation (3). From equations (2) and (3), we can see why galaxies with these combinations of properties are type 2 H II systems. Because of their low stellar surface densities, U_* is small; so a few luminous H II complexes can readily provide most of the warm L_{IR} observed by *IRAS*. Additional factors in dIm galaxies include their small optical diameters, very patchy distributions of stars and gas, and low metallicity levels, all of which will further reduce the efficiency with which dust absorbs stellar radiation and thus depress non–H II contributions to L_{IR}.

b) Complex Systems

In real galaxies a continuum will exist from purely H II–powered to purely GISRF–powered L_{IR}. Furthermore, a dichotomy may be present in GISRF–powered systems between those with cirrus-like spectral characteristics and those whose spectral properties are closer to the predictions of classical dust models (Helou 1986; Boulanger *et al.* 1988). The difficult problem in analyzing infrared observations of these complex types of galaxies is to disentangle which stellar population groups heat the dust responsible for L_{IR} observed by *IRAS*. We again limit our discussion to galaxies with low optical depths in the visual.

From equations (10) and (12) we see that the energy density of the GISRF, particularly at UV wavelengths, depends primarily on disk stellar luminosity and therefore on surface brightness. A correlation should therefore exist between disk surface brightness and infrared color temperature. In the simplest model, we assume that all irregular galaxies have the same stellar population temperature mixes and absorption optical depths through the disk. Then from the discussion in § IV*a*, the simplest model will have $U_* \propto l_{disk}$ (cf. eq. [10]), $T_D \propto l_{disk}^{1/5}$, and therefore $T_D \propto 0.08\mu_{disk}$, where μ_{disk} is the optical surface brightness in magnitude units. This simple scaling relationship is shown with data in Figure 7, where good agreement in slope is found; i.e., observed S_{100}/S_{60} color temperatures scale with surface brightness as expected if T_D is driven by the GISRF.

Demonstrating that the *values* of T_D predicted by simple models are consistent with observed values is a complex problem (e.g., Mezger, Mathis, and Panagia 1982; Mathis, Mezger, and Panagia 1983). A qualitative comparison can be made by noting that the GISRF in NGC 4449 resembles the Mathis *et al.* Galactic 5 kpc model, which gives temperatures well below 30 K, i.e., model dust temperatures appear to be too low. Thus, the true model relationship has the proper slope but falls above the observed trend in S_{100}/S_{60}. The origin of large luminosities from warm dust components outside H II regions in galaxies is still not fully understood, which hampers the analysis of global FIR *IRAS* observations of Irr and other classes of galaxies (Cox, Krügel, and Mezger 1986; Rowan-Robinson 1986).

A second complication in Figure 7 can be seen from the location of amorphous type 1 H II galaxies near the mean trend line (II Zw 40 is not plotted). Since we have argued that the GISRF is not the primary L_{IR} source in these systems, there is no physical reason for them to follow a surface brightness–T_D correlation. The two outlier galaxies, DDO 42 and DDO 50, on the other hand, illustrate the expected type of effect. These galaxies have overly warm dust temperatures because of the role of H II regions in producing L_{IR}. The interpretive problem that we have here is probably due to the statistical correlation of several galactic properties, including SFR, with optical surface brightness (see Fig. 6 of Hunter and Gallagher 1986). Thus our interpretation of the T_D–surface brightness plot in terms of the GISRF is not unique, and other possibilities exist, such as variations in the fraction of interstellar matter or near extremely low-density H II regions of the type invoked by Mezger and collaborators to explain Galactic warm L_{IR} emission.

Further progress would be possible if the component of L_{IR} from H II regions could be accurately separated from that due to the GISRF, which is not readily feasible from *IRAS* global photometric measurements. For example, the more than a factor of 2 range in the key S_{100}/S_{60} and $L_{IR}/L_{H\alpha}$ diagnostic ratios for individual H II regions eliminates any opportunity for the precise decomposition of galactic dust-heating sources (Thronson and Mozurkewich 1989). However, the general trends in Figures 2 and 7 for T_D to increase with both $L_{IR}/L_{H\alpha}$ and optical surface brightness suggest that GISRF is of increasing importance as a power source in systems with low T_D. DDO 47 is then a good example of a galaxy where most of the observed L_{IR} is due to the GISRF (cf. Hunter *et al.* 1986). Since these types of Irr's will generally have low L_{IR}/L_B and high S_{100}/S_{60}, they may be systematically underrepresented in samples of galaxies detected by *IRAS*.

c) Optically Thick Galaxies

If $\bar{\tau}_{H\alpha} > 1$, then FIR and optical properties of galaxies are no

longer simply connected (cf. Jura 1981; Soifer *et al.* 1987; Bushouse, Lamb, and Werner 1988; Trinchieri, Fabbiano, and Bandiera 1989). The discussion in § IV*b* indicates that galaxies with high $\bar{\tau}_{opt}$ are distinguished by optical luminosity deficiencies relative to L_{IR}; i.e., both L_{IR}/L_B and $L_{IR}/L_{H\alpha}$ will exceed values for optically thin galaxies. An examination of the optically thin Im and dIm galaxies in Table 3 suggests that optically obscured dust-heating sources are present in galaxies with $L_{IR}/L_B \geq 4$ and $L_{IR}/L_{H\alpha} > 100$. This energy source could be either stars or nuclear activity. Candidates for optically thick galaxies in our sample are the amorphous system Mrk 35 and the distant irregulars II Zw 23, III Zw 12, III Zw 43, and IV Zw 149.

None of these galaxies would be suspected of having substantial dust obscuration from routine optical measurements. They all have blue *UBV* colors and strong blue-region emission lines (e.g., [O II] λ3727 and Hβ). This is an effect described by Jura (1980), who noted that, if stars and gas are mixed, intensities (and colors) will depend on the source function (eqs. [10] and [12]). Since k_d is a more slowly varying function of λ than extinction optical depth, optically thick galaxies in which stars and gas are intermingled can have blue colors. Alternatively, when an obscuring screen of interstellar matter lies in front of the stellar sources, the radiative transfer problem resembles the extinction case and reddened colors will result (Elmegreen 1980).

The L_{IR}/L_B ratios in our optically thick candidate galaxies are 2–5 times the normal values. If L_{IR} is stellar-powered, then for these hot galaxies much of this difference will be caused by diminution of optical light rather than addition of L_{IR} (cf. Belfort, Mochkovitch, and Dennefeld 1987). *Optical observations underestimate stellar and emission-line luminosities by factors of* 3 *or more in these optically thick galaxies, thereby introducing major uncertainties into empirical determinations of evolutionary states.* Unfortunately, it is unclear at this time whether high and low optical depth blue galaxies can be distinguished from one another using standard, moderate signal-to-noise, visual spectrophotometric measurements.

All but one of the high optical depth systems is luminous, in agreement with the statistical correlation between L_{60} and L_{IR}/L_B described by Feigelson, Ishobe, and Weedman (1987). This is a natural result of the processes described by equations (11) and (12). Galaxies with large surface mass densities of stars and gas are most likely to be optically thick and thus to produce both high L_{60} and high L_{IR}/L_B.

VI. L_{IR} AND STAR-FORMATION RATES

The degree to which L_{IR} can be used as a measure of galactic SFRs is uncertain (e.g., Hunter *et al.* 1986; Thronson and Telesco 1986; de Jong and Brink 1987; Gallagher and Hunter 1987*a*; Persson and Helou 1987; Walterbos and Schwering 1987; Boulanger *et al.* 1988). Part of the difficulty centers on determining the appropriate time scale over which the SFR is averaged for each SFR indicator.

We will follow the approach developed by Gallagher, Hunter, and Tutukov (1984), where stellar-population parameters are associated with SRFs averaged over different time intervals. The differential SFR for a Salpeter IMF is then $d\dot{M} = 5.8\alpha_i M^{-2.35} dM\ M_\odot\ \mathrm{yr}^{-1}$, where the stellar mass range extends from $M_* = 0.1\ M_\odot$ to $M_u = 100\ M_\odot$. The L_{IR} in a given galaxy is then related to a star-formation rate α_{IR} by (Gallagher and Hunter 1987*a*)

$$L_{IR} = \alpha_{IR} \int_{M_*}^{M_u} (M^{-2.35}) \sum_j F_j(m)[\overline{L_j(m)t_j(m)}]dm\ . \quad (13)$$

Here M_* is the lower-bound zero-age main-sequence (ZAMS) stellar mass that significantly contributes to L_{IR}, the sum is over distinct evolutionary phases for each stellar mass m (cf. Tinsley 1980; Renzini 1981; Renzini and Buzzoni 1986), and F is an efficiency factor for converting stellar into FIR luminosity.

The value of α_{IR} in equation (13) and thus the SFR derived from L_{IR} depends strongly on both F and M_*. Since we expect most of the bolometric luminosity from irregulars to produce L_{IR} efficiently via dust absorption at infrared wavelengths, we choose $F = 0.5$ for the purpose of constructing simple models. From the existence of type 1 and type 2 H II galaxies, it is obvious that there is a range in M_*; therefore no universal conversion exists between SFRs and L_{IR}.

As an estimate for an H II galaxy, we take $M_* = 10\ M_\odot$, which corresponds to including only those stars with main-sequence effective temperatures of $T_e \geq 20{,}000$ K and lifetimes of $t_* \leq 2 \times 10^7$ yr.

Our model is based on a constant SFR from the epoch of observation t_0 to $t_0 + t_*$. The SFR from the model described by Gallagher (1987) is then

$$\dot{M}_{IR}(1) = 1.3 \times 10^{-43} E^{-1} L_{IR}\ M_\odot\ \mathrm{yr}^{-1}\ , \quad (14)$$

where E is given by equation (2). If we keep all other model parameters and assumptions the same and take $M_* = 2\ M_\odot$, which corresponds to $t_* \sim 10^9$ yr and $T_e \geq 10{,}000$ K, the derived SFR per unit L_{IR} decreases slightly:

$$\dot{M}_{IR}(2) = 1.0 \times 10^{-43} E^{-1} L_{IR}\ M_\odot\ \mathrm{yr}^{-1}\ . \quad (15)$$

Due to (1) the prominence of blue stars in the energetics of Irr galaxies and (2) the low visual optical depth assumption, which in effect requires that most dust be heated by UV light, L_{IR} is mainly sensitive to the total luminosity of upper–main-sequence stars. As a result, desired SFRs are not very sensitive to M_*, although the time interval over which the measured SFR is averaged is a sensitive function of M_*. Thus for H II galaxies, L_{IR} should provide information about SFRs over $\sim 10^7$ yr, while in a GISRF–powered system such as DDO 47, the averaging time is probably close to 10^9 yr.

SFR determinations also become difficult when mean visual optical depths are high in galaxies (Klein *et al.* 1986; Belfort, Mochkovitch, and Dennefeld 1987). In visual optically thick galaxies, evolved stars may begin to contribute to dust heating. The coefficient in equation (15) will then decrease by a factor of ~ 2, and the averaging time interval may increase to that characteristic of L_B in a constant SFR galaxy, $\sim 3 \times 10^9$ yr. SFRs based on equations (14) and (15) will then lead to overestimates.

The SFRs derived from luminosity measurements are model-dependent. It is therefore useful to compare SFRs determined from $L_{H\alpha}$, which depend on estimates of L_{Lyc} from young stellar populations, with those derived from L_{IR}. We use equation (14) and type 1 H II galaxies for this comparison, and $\dot{M}_{H\alpha}$ from Gallagher and Hunter (1987*a*). If these two SFR models are internally consistent and visual absorption levels are low ($\bar{\tau} \sim 0.3$), we predict $f_{IR}/f_{H\alpha} = 66$ (see eq. [14]). This is in reasonable agreement with the observed average value $\overline{f_{IR}/f_{H\alpha}} = 45$ for five type 1 H II galaxies (we omit Mrk 35, which is optically thick). The range of a factor of 3 in $f_{IR}/f_{H\alpha}$ in these galaxies provides a useful estimate of the uncertainties in *rela-*

tive SFR measurements that can be expected from the application of a single, universal model for conversions of global infrared or Hα luminosities into SFRs.

The agreement is also satisfactory for an average galaxy in the sample. Here the observed average is $f_{IR}/f_{H\alpha} = 54 \pm 5$ (mean error; excludes $f_{IR}/f_{H\alpha} > 100$) as compared with $f_{IR}/f_{H\alpha} = 53$ from equation (15). The half-power width in the observed distribution of $f_{IR}/f_{H\alpha}$ is again about a factor of 3. We have interpreted the tail to high $f_{IR}/f_{H\alpha}$ as an effect due to large optical depths in systems where f_{IR}/f_B is also high and as an effect of depressed current SFRs in cases such as DDO 47, where f_{IR}/f_B is low. Small values of $f_{IR}/f_{H\alpha}$ may similarly reflect microevolutionary differences occurring over small time scales during the development of individual young stellar complexes within galaxies. For example, the low value $f_{IR}/f_{H\alpha} = 13$ in the type 2 H II galaxy DDO 42 (NGC 2366) is certainly due to low $f_{IR}/f_{H\alpha}$ from the dominant giant H II region NGC 2363.

Several groups have suggested that many galaxies with blue *UBV* colors, such as those in this sample, are in "starburst" phases of enhanced star-forming activity (e.g., Thuan 1985; Lequeux 1986; Thronson and Telesco 1986). While there is no precise definition of a starburst, an operational definition is that the current SFR is more than 3 times the mean rate over the last few Gyr. Recognition of a starburst in all but extreme cases then depends on the choice of a model to determine recent evolutionary histories.

Gallagher, Hunter, and Tutukov (1984) developed a method of using L_B as an indicator of mean SFR averaged over 1–3 Gyr (see also Thronson and Telesco 1986; Gallagher 1987). For a constant SFR we predict $L_{IR}/L_B \sim 1$; for a burst, a conservative condition is $L_{IR}/L_B \geq 3$ (which corresponds to more than 3 times enhanced SFR because L_B also increases in a starburst). Bursting galaxies, however, will have near-normal $L_{IR}/L_{H\alpha}$. Note that it is then difficult to cleanly disentangle optical depth effects from SFR time variations in the optically thick distant Irr galaxies, but even so, indirect arguments suggest that some LBGs are likely to be in phases with enhanced SFRs (e.g., Belfort, Mochkovitch, and Dennefeld 1987; Krügel *et al.* 1988).

Among optically thin Im and dIm galaxies, only NGC 1012 and the type 1 H II galaxy NGC 1569 have burstlike characteristics; and, as discussed earlier, NGC 1012 may be heavily extincted. The remaining candidates for starbursts are all type 1 H II region amorphous galaxies, where optical properties are also consistent with time-variable SFRs (Gallagher and Hunter 1987*b*). *Therefore, most optically thin blue Irr galaxies do not experience high-amplitude time variations in SFRs over short* (<Gyr) *time scales. The blue Im systems are not experiencing starbursts and in this regard are similar to late-type spirals* (Trinchieri, Fabbiano, and Bandiera 1989). It is possible, as suggested by Belfort, Mochkovitch, and Dennefeld (1987), that most LBGs are in starburst evolutionary phases, but better probes of stellar populations in optically thick LBGs are needed to confirm this idea.

VII. SUMMARY AND CONCLUSIONS

We have presented *IRAS* 12, 25, 60, and 100 μm data for a sample of Irr galaxies which span a large range in star-formation activity. We find the following:

1. The dwarf, giant, and amorphous Irr's generally have similar infrared properties, although the dwarfs have somewhat lower L_{IR}/L_B. The LBGs, on the other hand, stand out as different with higher $L_{IR}/L_{H\alpha}$ and L_{IR}/L_B ratios and warmer S_{100}/S_{60} ratios.

2. The typical $L_{IR}/L_{H\alpha}$ ratios of most classes of Irr's, except for many of the LBGs, are low compared with those of spiral galaxies and are consistent with the Irr's being relatively transparent systems without large amounts of optically hidden star formation. Thus, $L_{H\alpha}$ is a good indicator of the current massive star formation in these systems.

3. Compared with spiral galaxies, the Irr's have similar L_{IR}/L_B ratios, warmer S_{100}/S_{60} ratios, cooler S_{25}/S_{12} ratios, and lower dust–to–H I gas mass ratios. This suggests that cirrus is less important in especially the nearby Im systems than in many spirals.

4. The temperature, dust–to–H I gas mass ratios, and L_{IR}/L_B ratios do not correlate with the metallicity of the ionized gas of the Irr's. We attribute the lack of correlation in L_{IR}/L_B to the ability of even low-metallicity galaxies to produce sufficient dust for $\tau > 1$ in the ultraviolet. Similarly, the absence of a clear dependence of IR color temperatures on metallicity suggests that grain composition is not a dominating factor in the spectral energy distribution in the 60–100 μm wavelength region.

5. For the Irr's we find a correlation between the infrared fluxes and both the Hα and the blue stellar fluxes, with the correlation with Hα being somewhat tighter. There is a trend toward higher L_{IR}/L_B ratios for higher surface brightnesses of Hα and blue stellar light. There is also a correlation between blue surface brightness and dust temperature, but not between Hα surface brightness and dust temperature.

6. Separating the GISRF from star-formation regions as sources for heating the dust from global properties alone is complicated. This is particularly so in galaxies such as the Irr's, where SFRs have been constant with time so that the GISRF and the current SFRs are themselves correlated. However, simple models are constructed consisting of the two primary sources of heating of dust—H II regions and the UV-dominated GISRF. H II region–dominated galaxies are expected to have $L_{IR}/L_{H\alpha} \sim 10$–30 and $S_{100}/S_{60} \leq 1.5$. A sample of Irrs dominated by a giant H II region is identified and found to be approximated by the models. The GISRF models predict that optically thin galaxies with higher UV surface brightness and lower dust absorption should have lower L_{IR}/L_B ratios and warmer dust color temperatures. The S_{100}/S_{60} ratios of Irr's are indeed warmer than for spirals; but, except for some of the dwarfs, the L_{IR}/L_B ratios are similar to those of spirals.

7. SFRs are derived from L_{IR}, and we find that, within the uncertainties, most nearby Irr's are not evolving via bursts of star formation.

8. Luminous Irr galaxies are likely to be optically thick and may be in starburst evolutionary phases. This view is consistent with the high densities of *IRAS* sources around luminous Irr's and with other evidence for involvement in galaxy-galaxy interactions which are potential triggers for starbursts.

9. The evolutionary states of luminous and other Irr galaxies that are potentially optically thick at visual wavelengths are not readily diagnosed from optical measurements. The LBGs are similar in many optical properties to the other Irr's but differ in terms of IR characteristics. Amorphous Irr's are a morphologically distinct subgroup but resemble normal Im systems in the IR. Spirals differ from Irr's in terms of many key optical and infrared properties but nevertheless have similar L_{IR}/L_B ratios compared with the Irr's. The differences in the

infrared between galaxies of similar optical properties and the similarities in the infrared between galaxies of different optical properties show that the infrared observations are important to a thorough understanding of the characteristics of star-forming galaxies.

We are grateful to all of the people involved in the *IRAS* project for an excellent infrared data base and to the people at IPAC for their assistance in extracting the data. This project was supported in part by grant 957275 from the National Aeronautics and Space Administration through the Jet Propulsion Laboratory as part of the *IRAS* General Investigator program and by the Lowell Observatory Research Fund.

REFERENCES

Belfort, P., Mochkovitch, R., and Dennefeld, M. 1987, *Astr. Ap.*, **176**, 1.
Bottinelli, L., Gouguenheim, L., and Paturel, G. 1982, *Astr. Ap.*, **113**, 61.
Boulanger, F., Beichman, C., Désert, F. X., Helou, G., Pérault, M., and Ryter, C. 1988, *Ap. J.*, **332**, 328.
Boulanger, F., and Pérault, M. 1988, *Ap. J.*, **330**, 964.
Burstein, D., and Heiles, C. 1984, *Ap. J. Suppl.*, **54**, 33.
Bushouse, H., Lamb, S., and Werner, M. 1988, preprint.
Cataloged Galaxies and Quasars Observed in the IRAS Survey. 1985, prepared by C. J. Lonsdale, G. Helou, J. C. Good, and W. Rice (Pasadena: JPL).
Carruthers, G. R., and Page, T. 1983, *Ap. J. Suppl.*, **53**, 623.
Chini, R., Kreysa, E., Krügel, E., and Mezger, P. G. 1986, *Astr. Ap.*, **166**, L8.
Code, A. D., and Welch, G. 1982, *Ap. J.*, **256**, 1.
Coleman, G., Wu, C.-C., and Weedman, D. 1980, *Ap. J. Suppl.*, **43**, 393.
Cox, P., Krugel, E., and Mezger, P. G. 1986, *Astr. Ap.*, **155**, 380.
Cox, P., and Leene, A. 1987, in *Star Formation in Galaxies*, ed. C. Persson (NASA CP-2466), p. 117.
de Jong, T., and Brink, K. 1987, in *Star Formation in Galaxies*, ed. C. Persson (NASA CP-2466), p. 323.
de Jong, T., Clegg, P. E., Soifer, B. T., Rowan-Robinson, M., Habing, H. J., Houck, J. R., Aumann, H. H., and Raimond, E. 1984, *Ap. J. (Letters)*, **278**, L67.
de Muizon, M., and Rouan, D. 1985, *Astr. Ap.*, **143**, 160.
Deutsch, L. K., and Willner, S. P. 1986, *Ap. J. (Letters)*, **306**, L11.
de Vaucouleurs, G., de Vaucouleurs, A., and Corwin, H. G. 1976, *Second Reference Catalogue of Bright Galaxies* (Austin: University of Texas Press).
Draine, B. T., and Lee, H. M. 1984, *Ap. J.*, **285**, 89.
Eastwood, K. 1989, preprint.
Elmegreen, D. M. 1980, *Ap. J. Suppl.*, **43**, 37.
Feigelson, E. D., Ishobe, T., and Weedman, D. W. 1987, *Ap. J. (Letters)*, **319**, L51.
Fisher, J. R., and Tully, R. B. 1981, *Ap. J. (Letters)*, **47**, 139.
Gallagher, J. S. 1987, *Mitt. Astr. Ges.*, **70**, 126.
———. 1989, in preparation.
Gallagher, J. S., and Hunter, D. A. 1987*a*, in *Star Formation in Galaxies*, ed. C. Persson (NASA CP-2466), p. 167.
———. 1987*b*, *A.J.*, **94**, 43.
Gallagher, J. S., Hunter, D. A., and Bushouse, H. 1988, in preparation.
Gallagher, J. S., Hunter, D. A., and Tutukov, V. 1984, *Ap. J.*, **284**, 544.
Gatley, I., Becklin, E. E., Hyland, A. R., and Jones, T. J. 1981, *M.N.R.A.S.*, **197**, 17P.
Gillett, F. C., Neugebauer, G., Emerson, J. P., and Rice, W. L. 1986, *Ap. J.*, **300**, 722.
Gordon, D., and Gottesman, S. T. 1981, *A.J.*, **86**, 161.
Grieve, G. R., and Madore, B. F. 1986, *Ap. J. Suppl.*, **62**, 427.
Haslam, C. G., and Osborne, J. L. 1987, *Nature*, **327**, 211.
Helou, G. 1986, *Ap. J. (Letters)*, **311**, L33.
Hodge, P. 1974, *Pub. A.S.P.*, **86**, 263.
Hunter, D. A. 1982, *Ap. J.*, **260**, 88.
———. 1984, *Ap. J. (Letters)*, **276**, L35.
Hunter, D. A., and Gallagher, J. S. 1985*a*, *Ap. J. Suppl.*, **58**, 533.
———. 1985*b*, *A.J.*, **90**, 80.
———. 1985*c*, *A.J.*, **90**, 1457.
———. 1986, *Pub. A.S.P.*, **98**, 5.
Hunter, D. A., Gallagher, J. S., and Rautenkranz, D. 1982, *Ap. J. Suppl.*, **49**, 53.
Hunter, D. A., Gillett, F. C., Gallagher, J. S., Rice, W. L., and Low, F. J. 1986, *Ap. J.*, **303**, 171.
IRAS Catalogs and Atlases, Explanatory Supplement. 1985, ed. C. A. Beichman, G. Neugebauer, H. J. Habing, P. E. Clegg, and T. J. Chester (Washington, DC: GPO).
IRAS Point Source Catalog. 1985, Joint *IRAS* Science Working Group (Washington, DC: GPO).
Israel, F. P., de Boer, K. S., and Bosma, A. 1986, *Astr. Ap. Suppl.*, **66**, 117.
Israel, F. P., and Koornneef, J. 1979, *Ap. J.*, **230**, 390.
Joy, M., and Lester, D. F. 1988, *Ap. J.*, **331**, 145.
Jura, M. 1980, *Ap. J.*, **238**, 499.
———. 1981, *Ap. J.*, **243**, 108.
Kennicutt, R. C. 1983, *Ap. J.*, **272**, 54.
Kinman, T. D., and Hintzen, P. 1981, *Pub. A.S.P.*, **93**, 405.
Klein, U., Heidmann, J., Wielebinski, R., and Wunderlich, E. 1986, *Astr. Ap.*, **154**, 373.
Koornneef, J. 1984, in *IAU Symposium 108, Structure and Evolution of the Magellanic clouds*, ed. S. van den Bergh and K. de Boer (Dordrecht: Reidel), p. 333.
Kraan-Korteweg, R., and Tammann, G. 1979, *Astr. Nach.*, **300**, 181.
Krügel, E., Chini, R., Kreysa, E., and Sherwood, W. A. 1988, *Astr. Ap.*, **193**, 211.
Lamb, S., Gallagher, J., Hjellming, M., and Hunter, D. 1985, *Ap. J.*, **291**, 63.
Lamb, S., Hunter, D., and Gallagher, J. 1989, *Ap. J.*, submitted.
Lequeux, J. 1986, *Highlights Astr.*, **7**, 557.
Lonsdale, C. J., Rice, W. C., and Bothun, G. D. 1987, *preprint*.
Low, F. J., *et al.* 1984, *Ap. J. (Letters)*, **278**, L19.
Mathis, J. S. 1973, *Ap. J.*, **186**, 815.
Mathis, J. S., Mezger, P. G., and Panagia, N. 1983, *Astr. Ap.*, **128**, 212.
Maucherat-Joubert, M., Lequeux, J., and Rocca-Volmerange, B. 1980, *Astr. Ap.*, **86**, 299.
Meaburn, J. 1980, *M.N.R.A.S.*, **192**, 365.
Mezger, P. G., Mathis, J. S., and Panagia, N. 1982, *Astr. Ap.*, **105**, 372.
Neugebauer, G., *et al.* 1984, *Ap. J. (Letters)*, **278**, L1.
Nilson, P. 1973, *Uppsala General Catalogue of Galaxies* (Uppsala: Uppsala Offset Center).
Pagel, B. E. J., Edmunds, M. G., Blackwell, D., Chun, M., and Smith, G. 1979, *M.N.R.A.S.*, **189**, 95.
Persson, C. J. L., and Helou, G. 1987, *Ap. J.*, **314**, 513.
Renzini, A. 1981, *Ann. Physique*, **6**, 87.
Renzini, A., and Buzzoni, A. 1986, in *Spectral Evolution of Galaxies*, ed. C. Chiosi and A. Renzini (Dordrecht: Reidel), p. 195.
Rowan-Robinson, M. 1986, *M.N.R.A.S.*, **219**, 737.
Sandage, A., and Brucato, R. 1979, *A.J.*, **84**, 472.
Sandage, A., and Tammann, G. A. 1981, *A Revised Shapley-Ames Catalog of Bright Galaxies* (Washington, DC: Carnegie Institution of Washington), Publication 635.
Scoville, N. Z., and Good, J. C. 1987, in *Star Formation in Galaxies*, ed. C. Persson (NASA CP-2466), p. 3.
Soifer, B. T., Houck, J. R., and Neugebauer, G. 1987, *Ann. Rev. Astr. Ap.*, **25**, 187.
Soifer, B., Sanders, D., Madore, B., Neugebauer, G., Danielson, G., Elias, J., Persson, C., and Rice, W. 1987, *Ap. J.*, **320**, 238.
Telesco, C. M., and Harper, D. A. 1980, *Ap. J.*, **235**, 392.
Thronson, H. A., and Bally, J. 1987, *Ap. J. (Letters)*, **319**, L63.
Thronson, H. A., Hunter, D. A., Telesco, C. M., Harper, D. A., and Decher, R. 1987, *Ap. J.*, **317**, 180.
Thronson, H. A., and Mozurkewich, D. 1989, *Ap. J.*, submitted.
Thronson, H. A., and Telesco, C. M. 1986, *Ap. J.*, **311**, 98.
Thuan, T. X. 1985, *Ap. J.*, **299**, 881.
Tinsley, B. M. 1980, *Fund. Cosmic Phys.*, **5**, 287.
Trinchieri, G., Fabbiano, G., and Bandiera, R. 1989, *Ap. J.*, submitted.
van den Bergh, S. 1959, *Pub. Dom. Ap. Obs. Victoria*, **2**, 147.
Viallefond, F., Donas, J., and Goss, W. M. 1983, *Astr. Ap.*, **119**, 185.
Viallefond, F., Goss, W. M., and Allen, R. J. 1982, *Astr. Ap.*, **115**, 373.
Walterbos, R. A. M., and Schwering, P. B. W. 1987, *Astr. Ap.*, **180**, 27.
Werner, M. W., Becklin, E. E., Gatley, I., Ellis, M. J., Hyland, A. R., Robinson, G., and Thomas, J. A. 1978, *M.N.R.A.S.*, **184**, 365.
Wesselius, P. R., van Duinen, R. J., de Jonge, A. R. W., Aalders, J. W. G., Luinge, W., and Wildeman, K. J. 1982, *Astr. Ap. Suppl.*, **49**, 427.
Wolfire, M. G., and Cassinelli, J. P. 1987, *Ap. J.*, **319**, 850.
Young, J. S., Keney, J. D., Tacconi, L., Clausser, M. J., Huang, Y.-L., Tacconi-Garman, L., Xie, S., and Schloerb, F. P. 1986, *Ap. J. (Letters)*, **311**, L17.

J. S. GALLAGHER and D. A. HUNTER: Lowell Observatory, 1400 West Mars Hill Road, Flagstaff, AZ 86001

F. C. GILLETT: NASA, Headquarters, Code EZ, Washington, DC 20546

W. RICE: California Institute of Technology, Mail Code 100-22, Pasadena, CA 91125